M.S. DISSERTATION

Preparation and characterization of ferroelectric $Hf_{0.5}Zr_{0.5}O_2$ films by RF sputtering method

RF 스퍼터 공법을 이용하여 증착한 $Hf_{0.5}Zr_{0.5}O_2$ 박막의 강유전성 확인 및 원인 분석

by

Young Hwan Lee

August 2016

DEPARTMENT OF MATERIALS SCIENCE AND ENGINEERING

COLLEGE OF ENGINEERING

SEOUL NATIONAL UNIVERSITY

Preparation and characterization of

ferroelectric $Hf_{0.5}Zr_{0.5}O_2$ films by RF sputtering method

Advisor : Prof. Cheol Seong Hwang

by

Young Hwan Lee

A thesis submitted to the Graduate Faculty of Seoul National University in partial fulfillment of the requirements for the Degree of Master of Science

Department of Materials Science and Engineering

August 2016

Approved

by

Chairman of Advisory Committee : Hyeong Joon Kim

Vice-chairman of Advisory Committee : Cheol Seong Hwang

Advisory Committee : Ho Won Jang

Abstract

HfO_2 is a dielectric material with a high dielectric constant, which provides an opportunity to replace the conventional Si as a gate dielectric material. Unlike conventional ferroelectrics with a perovskite structure, HfO_2 shows unprecedented ferroelectric behavior that arises from a non-symmetric orthorhombic lattice structure when doped by various dopants. Such behavior has been experimentally shown when deposited as a thin film by various deposition method, including atomic layer deposition, pulsed laser deposition, sol-gel method, to name a few. It is expected that only under certain condition does HfO_2 show ferroelectricity, and thus it is necessary to compare different deposition mechanisms and utilize the difference and experimental results to fully understand the atomic scale behavior of ferroelectricity within HfO_2.

In this paper, HfO_2 was deposited using a RF sputtering method with Zr as a dopant. RF sputtering method is more favorable than atomic layer deposition method in terms of the cost and the deposition time. Since sputtering imposes stress on the film upon deposition process which could likely act as a driving force for the realization of the non-symmetric lattice structure, it is expected to provide optimum condition for phase transition. Also, Zr possesses similar chemical characteristic with similar size as Hf, which could lead to a

favorable electrical behavior. HfO_2 and ZrO_2 oxide targets were co-sputtered simultaneously to fully provide the proper stoichiometry with O_2 reactive gas to avoid oxygen deficiency within the film.

The deposition conditions were varied with respect to reactive gas flow amount, power, working pressure, and annealing temperature. Zr doped HfO_2 showed different switching behavior and the deposition condition was optimized to result in the best ferroelectric behavior. To fully understand how such condition could affect the ferroelectric behavior, structural analysis and chemical analysis were conducted. As a result, the optimized condition for 10nm Zr doped HfO_2 using RF sputtering method was 130W and 195W for ZrO_2 and HfO_2 target power, respectively, with 1.33% of O_2 reactive gas and 600^{o}C annealing temperature for 1 minute under O_2 ambience. Different ferroelectric behavior is believed to result from grain size difference and oxygen vacancy concentration.

Keywords: HfO_2, ZrO_2, RF sputtering, ferroelectricity, oxygen vacancy, oxygen reactive gas, electrode oxidation, surface energy effect, grain size

Student Number: 2014-22540

Young Hwan Lee

Table of Contents

List of Tables

List of Figures

1. Introduction

Ferroelectric materials are polar materials, which possess two vectors of spontaneous polarization in the absence of an external electric field, and their orientation can be switched when electric field is applied. This non-volatile bipolar behavior has triggered interests among scientists and driven numerous research, seeking the possibility to utilize the very characteristic and mechanism for the next generation nonvolatile memory devices.

Their atypical behaviors can be utilized in many aspects such as ferroelectric random access memory (FRAM)[1-2] or ferroelectric field effect transistor (FeFET)[3], to name a few. Most of the early researches were based on the materials system based on a perovskite structure in which anion at the center of the lattice fluctuates towards the applied filed direction which spontaneously produces the dipole between the cation and the anion. However, the difficulties still remain because the usage of Pb from $Pb(Zr,Ti)O_3$ (PZT) which is the main perovskite structure of interest with large polarization value, was not eco-friendly, and as the technology evolved, it required thinner film. This thin structure provides difficulties in fabrication process for perovskite structured materials.[4] Perovskite ferroelectrics also have other problems such as ferroelectric size effect, degradation by thermal budget during crystallization,

small bandgap, and poor interfaces with Si.[5-6]

However, it was recently found that HfO_2, which holds a non-perovskite structure, exhibits a ferroelectric behavior at a thickness of less than 10nm scale.[7] Considering the importance of scaling down of the memory devices, the intensive research on the fundamental properties of ferroelectric HfO_2 is highly encouraging. HfO_2 material system not only avoids the problems of conventional ferroelectric perovskite materials, such as PZT or $SrBi_2Ta_2O_9$ (SBT), but also produces large polarization value at thickness of less than 10nm.[7] HfO_2 is also compatible with the conventional Si technology and appropriate for three-dimensional capacitors.[8]

HfO_2 based thin film shows ferroelectricity only under limited conditions. When doped with various dopants such as Si, Y, Al, or Zr, HfO_2 shows hysteresis curve and its ferroelectricity is believed to result from the formation of non-centrosymmetric $Pbc2_1$ orthorhombic phase (o-phase). [9-12] Different dopant type shows ferroelectricity under limited dopant concentration and produces different ferroelectric behavior with different spontaneous polarization values.

Out of all the dopants, Zr is a promising dopant since its chemical properties are almost identical to that of Hf. It has been reported that dopant size affects the property of HfO_2.[13] Since Zr atomic size is very similar to Hf, it does not produce radical volumetric change within the lattice and shows wider

range of composition to show ferroelectricity.[11]

In this study, co-sputtering method was used with oxide targets to fabricate Zr doped HfO_2 thin film. In-plane strain within the tetragonal phase (t-phase) is one of many influencing factors to achieve non-symmetric o-phase that is likely to occur from Volmer-Weber-type growth, which is usually observed during sputtering.[8] Oxygen flow, target power, working pressure, and annealing temperature was varied to optimize the processing condition for the best ferroelectricity. After optimization, comprehensive analysis were conducted to understand the atomic scale behavior for doped HfO_2 to produce its ferroelectricity.

2. Literature

2.1. Sputter Deposition Technique

Sputter deposition is one of the most widely used thin film deposition techniques and has been used for decades. It holds advantages such as fast deposition rate, optimum control of the film composition and microstructure, and comparatively cheap manufacturing cost. Since different deposition method provides different growth mechanism, the experimental results using sputtering could act as a comparison parameter to qualitatively understand the origin of the atomic scale domain formation of HfO_2, which would be a great motivation to use a sputter.

Sputter deposition mechanism belies on physical vapor deposition (PVD) method, where a molecule or an atom is physically separated from the target by bombardment of Ar ion atoms and gets deposited onto the film directly. Fig. 1 shows a schematic diagram of how sputtering mechanism works. As the target is negatively biased, drifting electrons inside the chamber will flow towards the substrate, and as it moves, it will bombard with floating Ar atoms and produce Ar+ ions. Ar+ ions would then move towards and bombard the negatively biased target, and removed target atoms would fly and deposit onto the substrate.

There are some deposition factors to influence the deposition rate. Fig 2. shows how each deposition condition influences the deposition rate. The deposition rate is closely related to the grain size and the density of the film. Therefore, it is necessary to carefully control the deposition condition to meet the proper film quality needs.

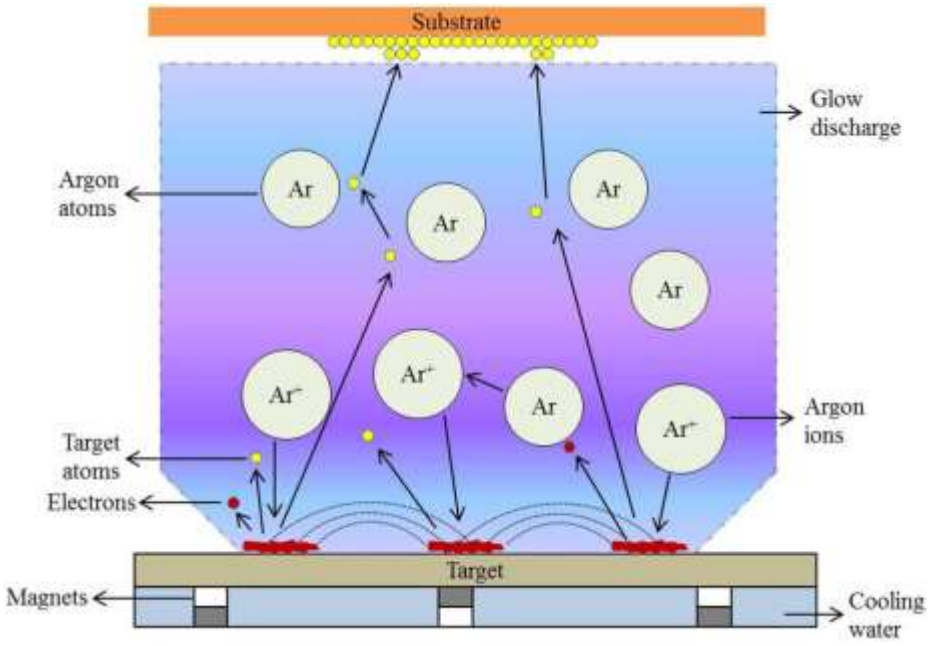

Figure 2. 1 The schematic diagram of RF magnetron sputtering[14]

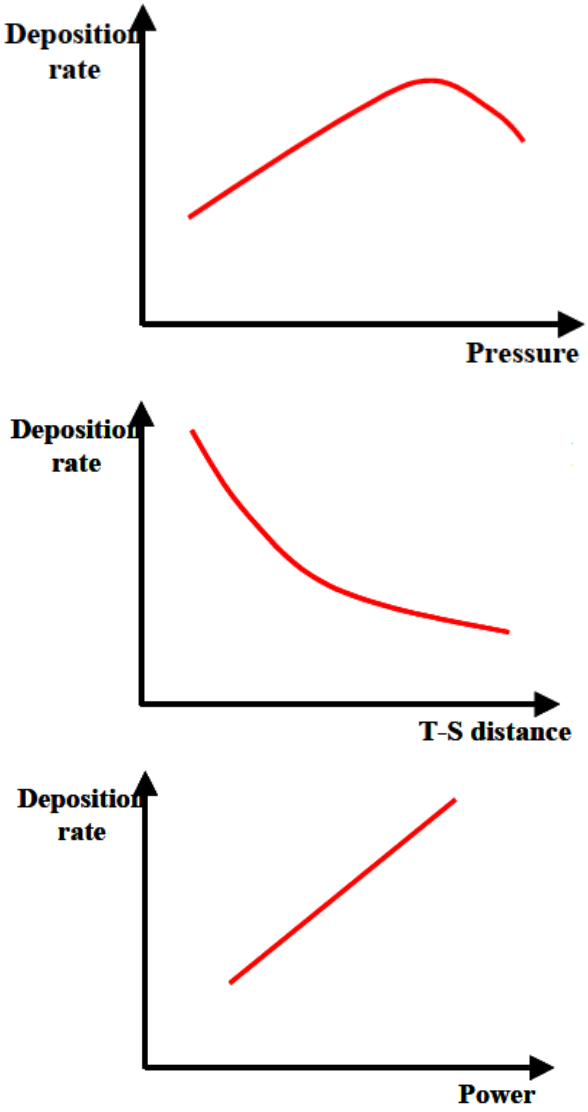

Figure 2. 2 Different deposition conditions such as (a) pressure, (b) target-substrate distance, and (c) power biased on targets, influencing the deposition rate.[15]

2.2. Conventional Ferroelectric Materials

It is usually of interest to consider the polycrystalline ferroelectrics because of the difficulty to modify compositions for single crystals. Realization of the quasi bi-stable polarization requires a certain lattice structure. It is important to consider the geometry of the materials since it can lead to very different properties of films with respect to bulk materials and should be taken into account in advance when modelling devices.

Ferroelectric materials experience a structural phase transition at a boundary called Curie temperature, above which they lose polarity and show non-ferroelectric (paraelectric) phase, below which they show ferroelectric phase. Conventional ferroelectric materials usually possess a perovskite structure, where cation at the center of the lattice fluctuates towards the direction of which external electric field is applied. When the poling occurs, it creates different polarization domain, which altogether aids in the formation of spontaneous polarization. Perovskite crystals have the general formula of ABO_3 where the valence of A cations is from +1 to +3 and B cations from +3 to +6. Fig. 2.3 shows the widely known ferroelectric materials PZT with a perovskite structure. Within the structure, Zr or Ti atom fluctuates to create dipole within the lattice upon applying electric field. This fluctuation is possible due to a weak bonding between Zr or Ti atom and oxygen atom. When the switching occurs, it creates a hysteresis curve due to remanent polarization (P_r), a polarization value when

no electric field is applied. This P_r, is a representative value to express the quality or memory window of ferroelectric materials when utilized in devices such as FRAM. When the polarization switching occurs, it is necessary to apply above certain amount of electric field, or coercive field (E_c), to overcome the energy barrier between two stable polarization states. PZT, for instance, has high P_r value of 20~30 $\mu C/cm^2$ at a thickness of ~200~600nm with coercive field of 50kV/cm.[16] However, PZT has an intrinsic environmental issue since Pb is not eco-friendly and is a hazardous waste. Also, PZT loses its P_r value dramatically as it is scaled down, which could act as a demerit to be used for modern memory applications.

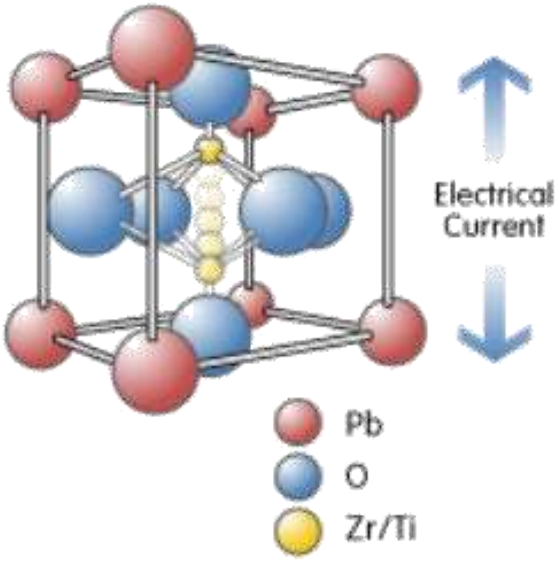

Figure 2. 3 Lattice structure of $Pb(Zr:Ti)O_3$, a widely known conventional perovskite ferroelectric material.[12]

2.3. Properties of doped HfO_2 and $(Hf:Zr)O_2$

HfO_2 is a dielectric material and shows a monoclinic phase (m-phase) at low temperature, which does not show any ferroelectricity and is referred to as paraelectric. At high temperature, HfO_2 transforms to a t-phase, which is also paraelectric. It is interesting that HfO_2 with different phases prepared under different circumstances possess various dielectric constant with ~20 for m-phase and ~35 for t-phase.[7] Therefore, the preparing condition should be engineered to achieve ideal material with proper characteristic. When there exists external force such as high temperature, dopants or stress, the material undergoes phase transformation to unprecedented o-phase with dielectric constant of ~30.[7] The very phase is non-symmetric which is believed to be the cause of the origin of the ferroelectric behavior. The phase transformation and its respective dielectric constant is depicted in Fig. 2.4.

Formation of the o-phase is viable under limited condition, and only under certain high-pressure does o-phase become a stable phase. Lowther et al. reported that the phase transition from the m-phase HfO_2 to o-phase is viable under hydrostatic pressure of 3-4 GPa based on the theoretical calculation.[17] However, such pressure and corresponding strain are difficult to arise within thin films. Thin film would rather be subjected to two dimensional tensile or compressive stress or strain depending on the deposition condition and annealing condition, due to local stress from the lattice mismatch or the thermal

expansion coefficient difference between the thin film and the substrate.

There is another report on the phase transition from t-phase to o-phase using MgO doping on ZrO_2, which was the first realization of the o-phase.[18] The transformation resulted from the compressive stress along a- and b- axis of the t-phase and tensile stress along c- axis. According to the literature, about ~760 MPa tensile and ~50 MPa compressive stress were necessary for the transition, which could be easily achieved within thin films.[18] Before further discussion, the axis difference between the t-phase and the o-phase should be considered. The longest axis for t-phase is c-axis, whereas that of the o-phase is a-axis. The c-axis of the t-phase is elongated and becomes a-axis for the o-phase. As a result, the o-phase would have the polarization towards the c-axis direction, which would be parallel to the film surface direction.[8]

Dopants introduce certain stress effect to the host material. When dopants replace Hf atom, different size of the dopants causes structural deformation which arises from the change in bond length and angle or coordination number.[13] Lattice distortion would, as a result, change the most stable phase. If the radii of dopants are smaller than those of Hf atoms, then it would likely shorten the dopant-oxygen bonds. Since Hf-O bond length in t- phase is already short, dopants would create a little distortion and result in the t-phase formation. On the other hand, dopants with greater radius than that of Hf atom would

elongate the bonds around O atoms. Since m-phase and t-phase contain several short Hf-O bonds than the cubic phase (c-phase), the large dopants will make the c-phase more stable.[13]

Both Hf and Zr possess m- phase under bulk structure. When the thickness of the film decreases, however, both materials go through the phase transformation. With decreasing thickness, the grain size also decreases, which is closely related to the surface energy. Due to the surface energy consideration, critical value of the grain size at which transformation from m-phase to t-phase occurs is ~5nm and ~30nm for HfO_2 and ZrO_2, respectively.[19] Unlike other dopants, Zr atom has a similar size of the radius and would not change the Hf-O bond length by much. In fact, due to the size similarity, ferroelectricity is shown over wide range of composition compared to other dopants concentration. As mentioned above, non-symmetric o-phase formation is required for the polarization to occur. The direct transition from m-phase to o-phase is hindered because the crystalline structures for each phase are much different. Pure HfO_2 usually favors monoclinic phase and it contains grain size that is above the critical grain size limit for transition to t-phase to occur. Zr atom makes this transition easier since polycrystalline ZrO_2 easily shows t-phase, especially on TiN, and has grain size that is smaller than the critical value.[4] As a result, Zr dopant will aid HfO_2 in transition from t-phase to o-phase by adjusting the grain size that will be suitable for the phase change.

There have been reports on the dependency of the polarization hysteresis on dopant concentration. Pure HfO_2 and ZrO_2 show m-phase and t-phase respectively at a thickness of ~10nm. When Zr dopant on HfO_2 is varied, it starts with slanted hysteresis with smaller P_r when stoichiometry of Hf is larger than Zr. As Zr dopant increases, the hysteresis gets larger with higher P_r; and when Hf to Zr ration exceeds 1:1, the film starts to show antiferroelectric behavior.[11] Fig. 2.5 shows summarizes the different hysteresis result depending on Zr dopant concentration. When Hf is dominant, m-phase is dominant within the film, while Zr dominant thin film possess more of t-phase, leading to antiferroelectric behavior. Therefore, it is necessary to carefully control the dopant concentration to achieve high P_r.

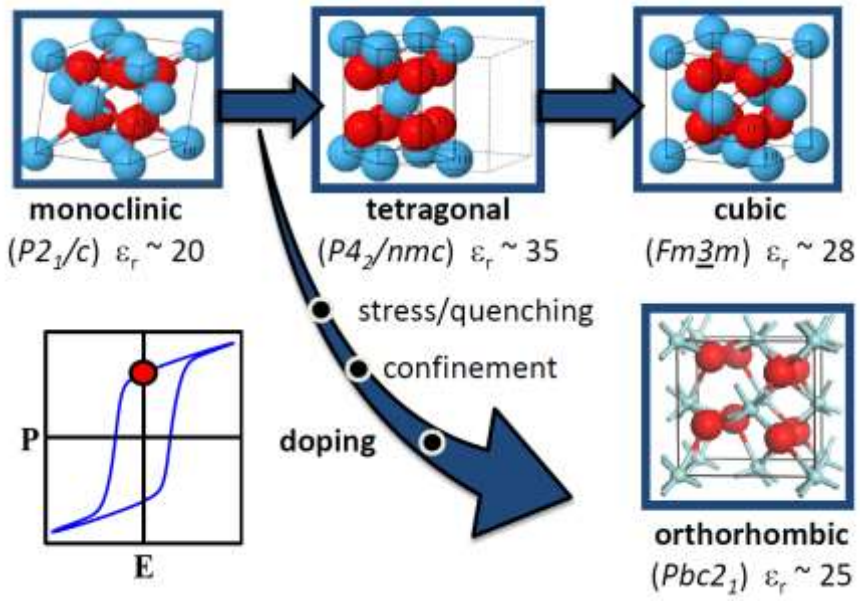

Figure 2. 4 Centrosymmetric polymorphs of HfO_2 and orthrhombic phase formation due to stress/quenching, confinement, or doping.[17]

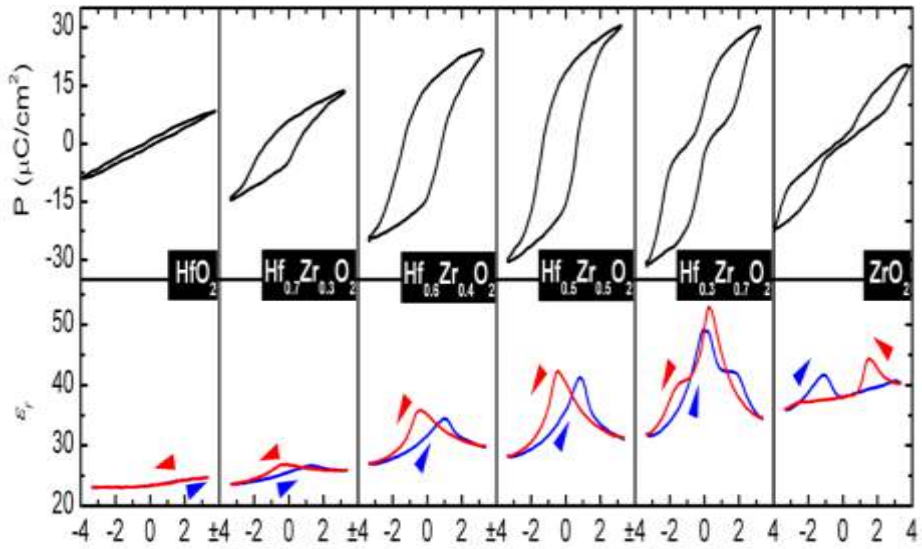

Figure 2. 5 Comparison of hystersis curves of $Hf_xZr_{1-x}O_2$ thin film depending on different Zr dopant concentration[11]

2.4. Other Factors to Influence the Ferroelectricity

Non-symmetricity from the o-phase is the critical requirement of the realization of the ferroelectricity. However, there are other conditions to be met in order to achieve stable high bi-stable polarization. Factors like interface with electrodes, annealing conditions, thickness and the grain size could affect the formation and the stabilization of the o-phase.[7, 20-22]

It is reported that the interface between the ferroelectric oxide films and the electrode is important not only to induce high P_r but also to achieve enhanced fatigue behavior. Ferroelectric HfO_2 has been deposited on/under various bottom electrode (BE) and top electrode (TE), including RuO_2, Pt and Ir.[22-24] Although the ferroelectricity is well formed under these electrodes, the best results were reported so far when the oxide thin film was deposited on the TiN BE.[25] TiN is a polycrystalline without any preferred orientation. The polycrystalline structure of the BE influences the growth and orientation of grains during thermal annealing process. When Gd doped HfO_2 thin film was deposited on TiN BE, there was not any abrupt change in crystal structure between the oxide film and the electrode.[25] It was expected that TiO_xN_y layer was formed since TiN easily oxidizes, scavenging oxygen from Gd:HfO_2 layer and forms oxygen vacancies within the oxide layer. These external factors such as oxygen vacancies and interface quality can strongly influence the quality of the film and electrical behavior.

Different annealing conditions may also result in distinct polarization behavior. Since the BE is polycrystalline TiN, when the oxide thin film is deposited on top, it has an amorphous structure. Different thermal annealing condition affects the domain growth behavior within the film, and at the same time changes the interface layer between the oxide film and the electrodes. Shimizu et al. reported that although no significant difference was observed for $Hf_{0.5}Zr_{0.5}O_2$ (HZO) film annealed under N_2 and O_2 ambient at 700ºC for 10 minutes, heat-treated ambient affected the crystallized phase of the film.[21] Their another reported showed that different annealing temperature and time resulted in large different in polarization-electric field hysteresis,[22] shown in Fig. 2.6. The discrepancy between two results, although the same material used, arose from different TEs and BEs, indicating that annealing condition affects the condition of the electrodes, leading to difference in electrical behavior of thin film. Therefore, under limited thermal budget as well as dopant content does HfO_2 attain o-phase to show ferroelectricity, which is well depicted in Fig. 2.7.[26]

Ferroelectric behavior of doped HfO_2 is also dependent on thickness and grain size of the film as well.[7] Thickness of the film and the grain size are highly related. As the film thickness gets thicker, the grain size increases due to the nucleation and growth behavior continues as the film thickness grows. When the surface free energy decreases, it is possible to achieve t-phase without achieving high temperature.[27] Park et al. reported that when thickness of the

film gets thicker, large grains form leading to m-phase formation due to high surface energy of the m-phase than that of the t-phase.[7] This dominant m-phase formation led to smaller P_r due to its paraelectricity. When the thickness was smaller than 10nm, the grain size was small enough to stabilize the metastable t-phase. The corresponding polarization value decreases due to the formation of the o-phase by free energy and surface energy consideration and possibly from t-phase to o-phase transformation under high electric field.[7] Fig 2.8 well summarizes such behavior, and the thickness of the film should be considered as one of the factor to achieve large P_r.

The same theory also applies when HZO thin film is deposited on Pt, where its grain size well exceeds the size of 20nm leading to large grain size and the formation of the m-phase. In addition, it is well known that the thin film orientation is easily influenced by the bottom layer. Due to similar lattice structure between HfO_2 and ZrO_2, (111) oriented HZO film is expected to form on (111) oriented Pt substrate. T-phase grains with (111) orientation is believed to be inappropriate for the o-phase formation because tensile strains along a-, b-, and c-axis are almost equivalent, resulting in isotropic-like strain.[8] According to the anisotropic strain consideration already discussed in section 2.3, combined with grain size consideration, ferroelectricity for (111) oriented HZO is highly unlikely, shown in Fig. 2.9.

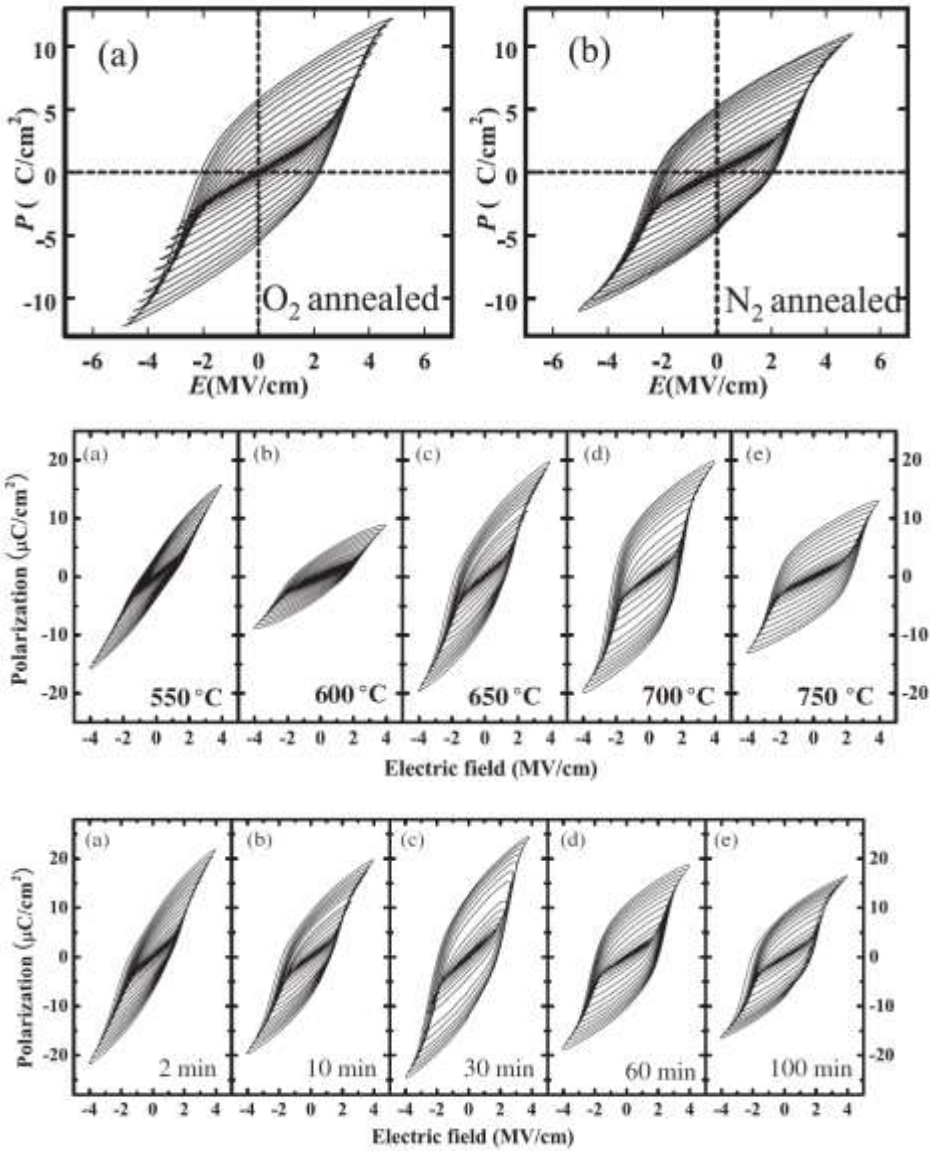

Figure 2. 6 Different annealing condition (annealing ambience, tempearture and time) affecting the hystersis behavior of $Hf_{0.5}Zr_{0.5}O_2$ thin film.[21-22]

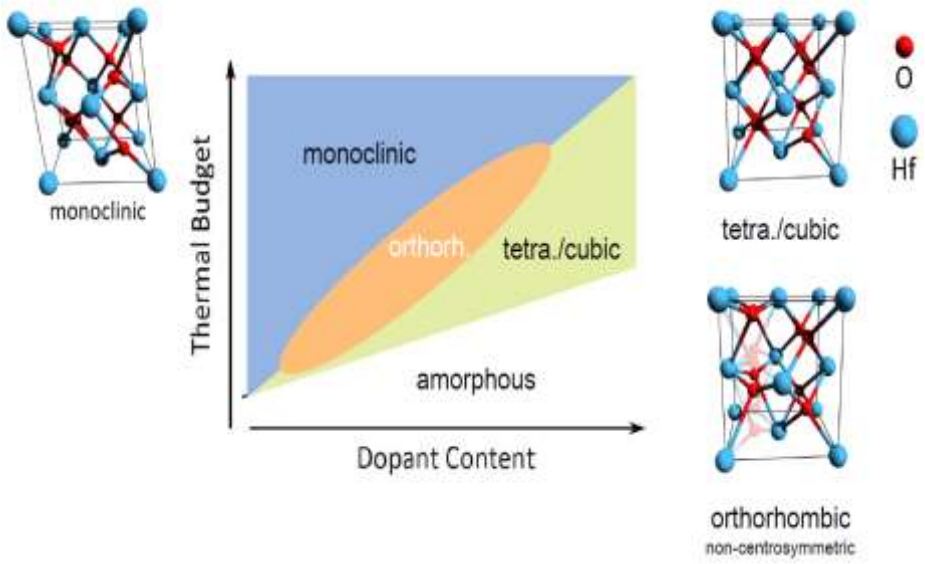

Figure 2. 7 Dependence of stable phase of HfO_2 on thermal budget and dopant content.[26]

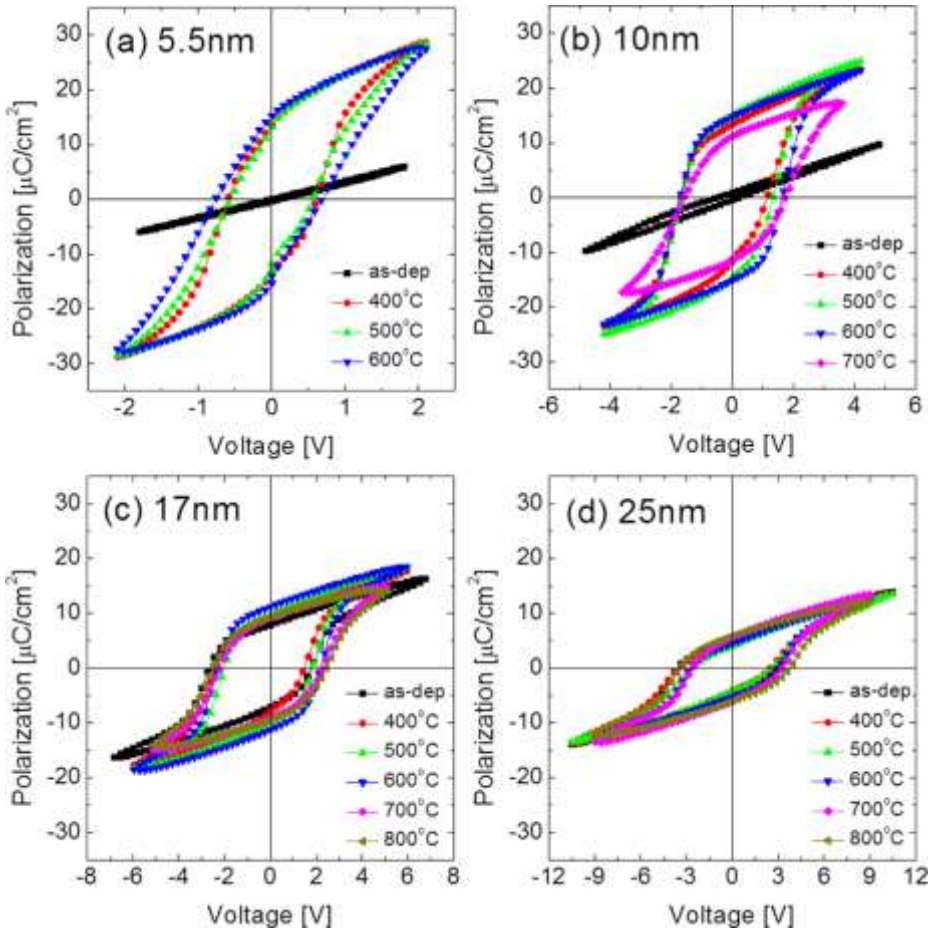

Figure 2. 8 Hystersis curve with different remanent polarization value depending on the the thickness of $Hf_{0.5}Zr_{0.5}O_2$ film.[7]

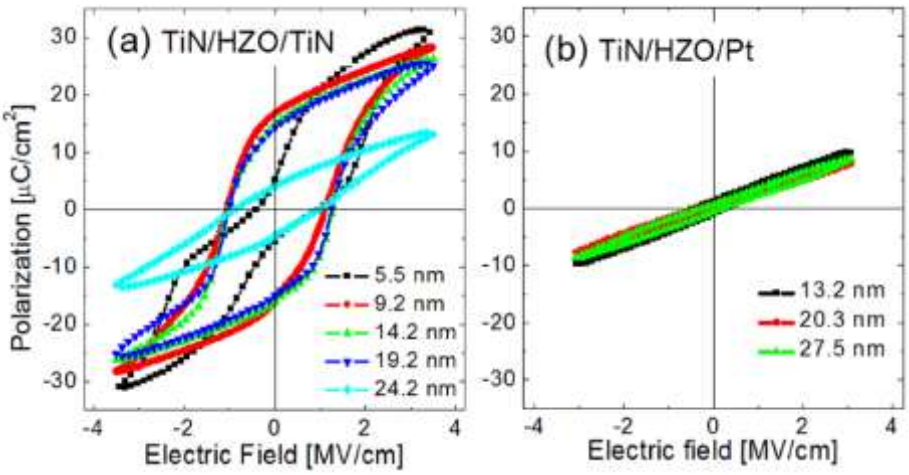

Figure 2. 9 P-E characteristics of the $Hf_{0.5}Zr_{0.5}O_2$ capacitors with various thickness on (a) TiN and (b) those on Pt.[8]

3. Experimental

3.1. Oxide targets co-sputtering of thin (Hf:Zr)O_2 film

HZO thin film was deposited on a TiN/Ti/SiO_2/Si substrate by RF sputtering method. Fig. 3.1 shows the schematic diagram of RF magnetron sputtering condition using HfO_2 and ZrO_2 oxide targets. TiN was sputtered on a SiO_2/Si substrate with Ti adhesion layer using a DC reactive magnetron sputter. The thickness of each layer for TiN, Ti, SiO_2 was 50nm, 5nm, and 100nm, respectively. Approximately 11nm of HZO thin film was deposited by RF magnetron co-sputtering using a 3 in-diameter HfO_2 and ZrO_2 targets at room temperature. The distance between the target and the substrate is about 12cm. The sputtering process was conducted with a working pressure of 1mTorr and RF power was varied to set the composition of 1:1 ratio. The reactive gas percentage was varied from 0 to 3.33% of O_2 and the TE. Pt (30nm thickness)/TiN (5nm thickness) TE was deposited by DC magnetron sputtering through a shadow mask with 300μm hole diameter. After TE deposition, the post-metallization-annealing (PMA) was conducted under O_2 atmosphere using a rapid thermal annealing (RTA) for film crystallization. Annealing temperature was varied from 550°C to 650°C by 50°C interval and annealing time was also varied from 30 seconds to 5 minutes.

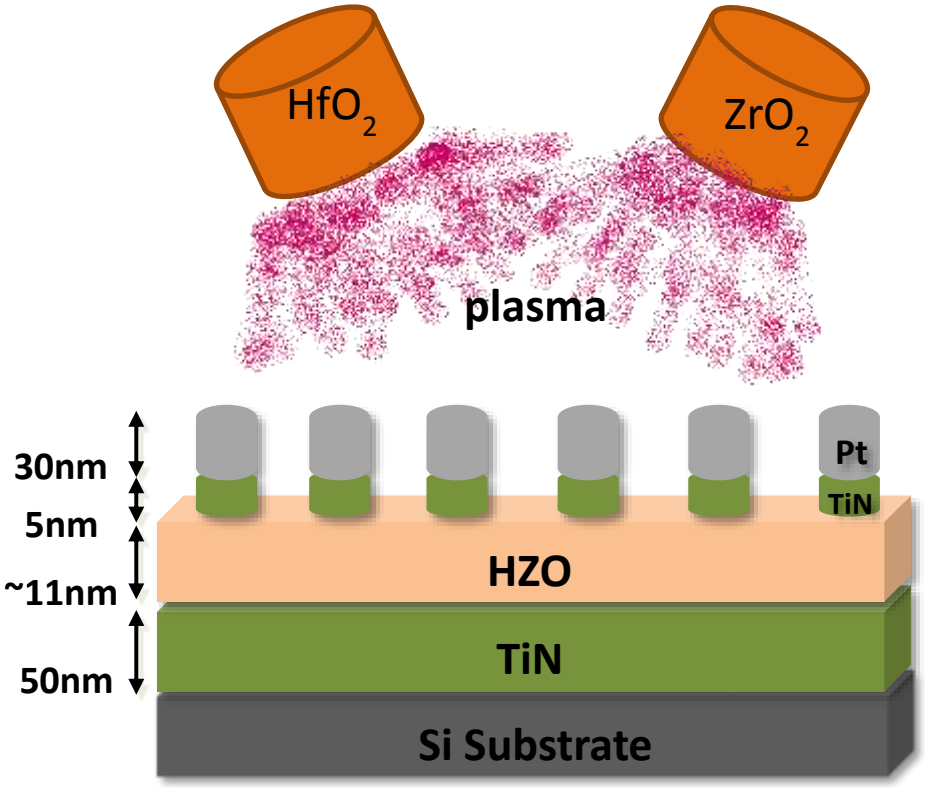

Figure 3. 1 Schematic diagram of RF magnetron sputtering using HfO_2 and ZrO_2 as two co-sputtering target. ~11nm $Hf_{0.5}Zr_{0.5}O_2$ thin film was deposited on 50nm thick TiN bottom electrode and Pt/TiN top electrode was deposited with a shadow mask of 300um hole diameter.

3.2. Electrical Measurement and Structural Analysis

The composition and the film thickness of HZO were examined by X-ray fluorescence analysis (Quant'X, Thermo SCIENTIFIC) and ellipsometry(L-116d, Gaertner), respectively. The grain size and the cross sectional image were obtained by scanning electron microscope (SEM). The crystal structure of the HZO film was examined using an X-ray diffractometer (X'pert Pro, Panalytical) by grazing-angle incidence X-ray diffraction (GIXRD, incidence angle=0.5). For electrical characterization, the polarization-electric field (P-E) characteristics were measured using a ferroelectric tester (TF Analyzer 2000, Aixacct Systems) in virtual mode. Triangular bipolar pulses with a 1kHz frequency were applied to the TE with the BE grounded. The dielectric constant-electric field (ε_r-E) characteristics were measured using an impedance analyzer (4194A, Hewlett-Packard, at the AC bias frequency of 10 kHz and amplitude of 50 mV).

4. Experimental Results and Discussions

4.1. Realization of Ferroelectricity of Sputtered HZO film

Using metal targets was first attempted to deposit HZO thin film. Power, working pressure, and reactive gas partial pressure were varied to achieve ideal HZO thin film with 1:1 Hf:Zr stoichiometry. However, the leakage problem could not be fixed even after annealed in oxygen ambience. Annealing in N_2 ambience and O_2 ambience created different film quailty as can be seen in Fig. 4.1. Although leakage behavior was enhanced a bit when oxygen was supplied during annealing, which can be seen in Fig. 4.2, no switching was observed. There seems to be one switching peak under the condition 80W/150W for Hf/Zr power (highlighted with green) in the current-voltage data, shown in Fig. 4.2 (b). Although further investigation was not conducted, enhanced electrical property is expected with oxide targets.

It is intersting to note that the results are quite different from what has been reported earlier in which no effects from annealing temperature and condition were found.[21] The difference could rise from different film deposition method. Sputtering is a physical vapor deposition process, where the film quality can be influenced by mechanical energy of bombarding particles; whereas, T. Shimizu et al. depsoited the same material by metal-organic chemical vapor depostion (MOCVD).[21] Also, since TE and BE are TiN which easily oxidizes, annealing

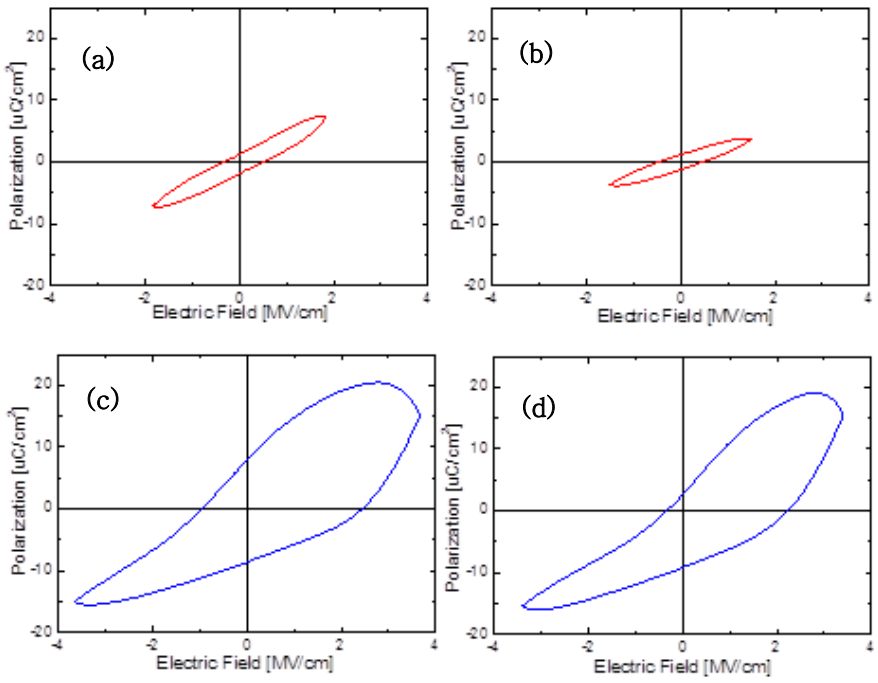

Figure 4. 1 Polarization-electric field graph of $Hf_{0.5}Zr_{0.5}O_2$ thin film prepared using metal targets under following conditions. (a) Hf/Zr=150/190W (b) Hf/Zr=80/105W, both annealed under N_2 ambience, (c) Hf/Zr=150/190W (d) Hf/Zr=80/190W, both annealed under O_2 ambience.

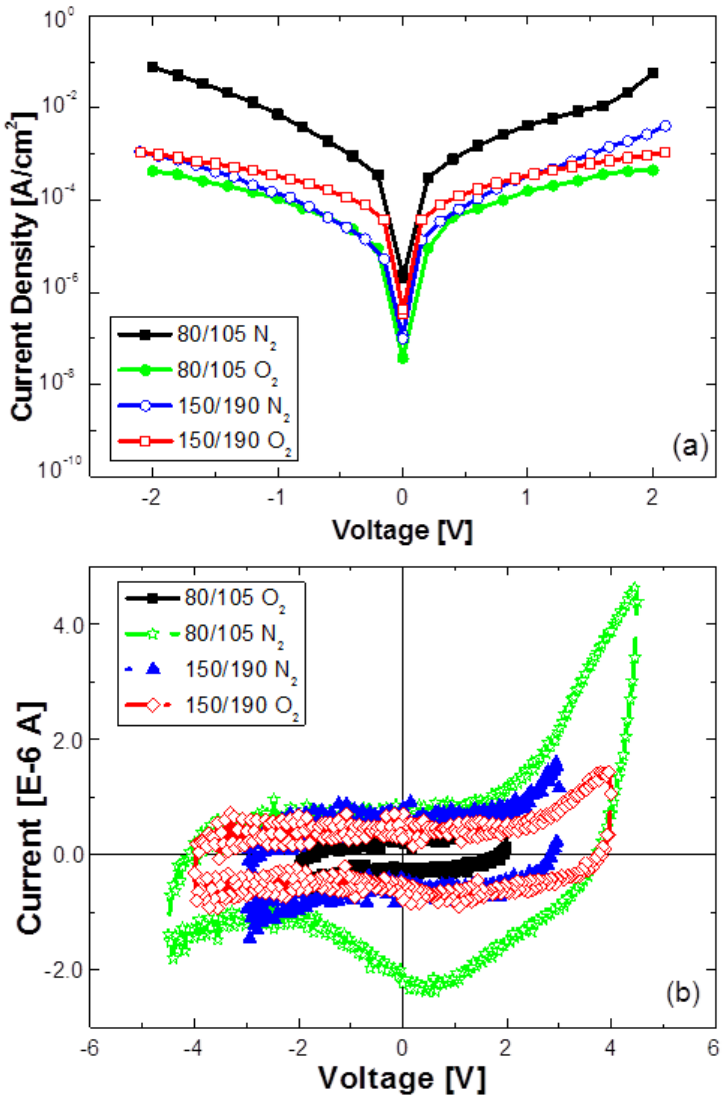

Figure 4. 2 Current-voltage data of $Hf_{0.5}Zr_{0.5}O_2$ thin film using different power under different annealing ambience. (a) shows the log scale and (b) shows the data using triangle pulse at 1kHz.

in O_2 ambience must create different interface layer than that annealed in N_2.

Fig. 4.3 shows the IV characteristic behavior of HZO films deposited using different target under different annealing condition. Although more experiments and planned out explanations are required to fully explain the difference, it can be easily seen that HZO film prepared using metal targets produced less favorable results. Again, since the samples prepared using oxide targets showed better current-voltage (I-V) behavior, favorable outcome could be expected.

Experimental data shows that only under limited condition does films deposited using oxide targets show ferroelectricity. Interesting event occurred when pre-sputtering was conducted using Hf metal target. To reach the base pressure below ~$7.0x10^7$ torr, pre-sputtering using metal target was necessary to remove any unwanted substances. The film deposited after pre-sputtering showed much different structure formation than that of the film under normal condition without any sputtering with metal target, as shown in Fig. 4.4. In this figure, it can be easily seen that o-phase around 30.5^o 2θ value is well formed with high intensity although considerable amount of m-phase has also been created. It can be deduced from this experiment that unintentionally, the metal target atoms got stuck on the chamber wall which took away some of the oxygen atoms that was necessary during the HZO deposition as a reactive particle. When the capacitance-voltage curve was plotted, as shown in Fig. 4.5

(a), the film successfully showed the butterfly figure, which indicates the successful polarization switching. Fig. 4.5 (b) shows that anealing in N_2 condition creates more leakage problem and that O_2 annealing is indispensable. Although Fig. 4.5 (c) does not show a clean hystersis behavior, oxygen deficient condition must be achieved during deposition of the HZO film while O_2 annealing is necessary to avoid large leakage problem.

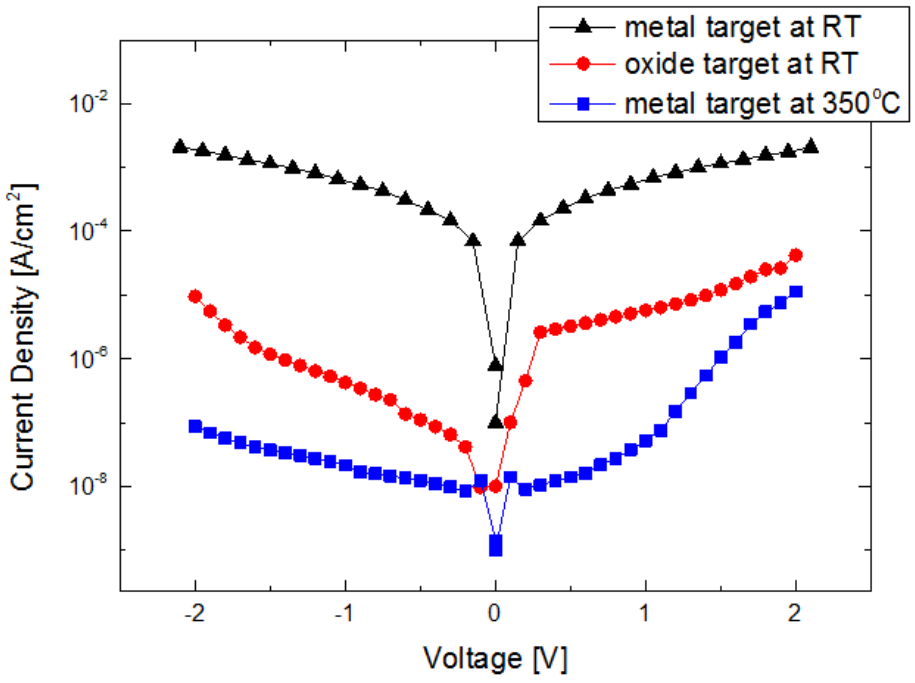

Figure 4. 3 I-V data of Zr doped HfO_2 prepared using oxide targets and metal targets at room temperature and 350°C.

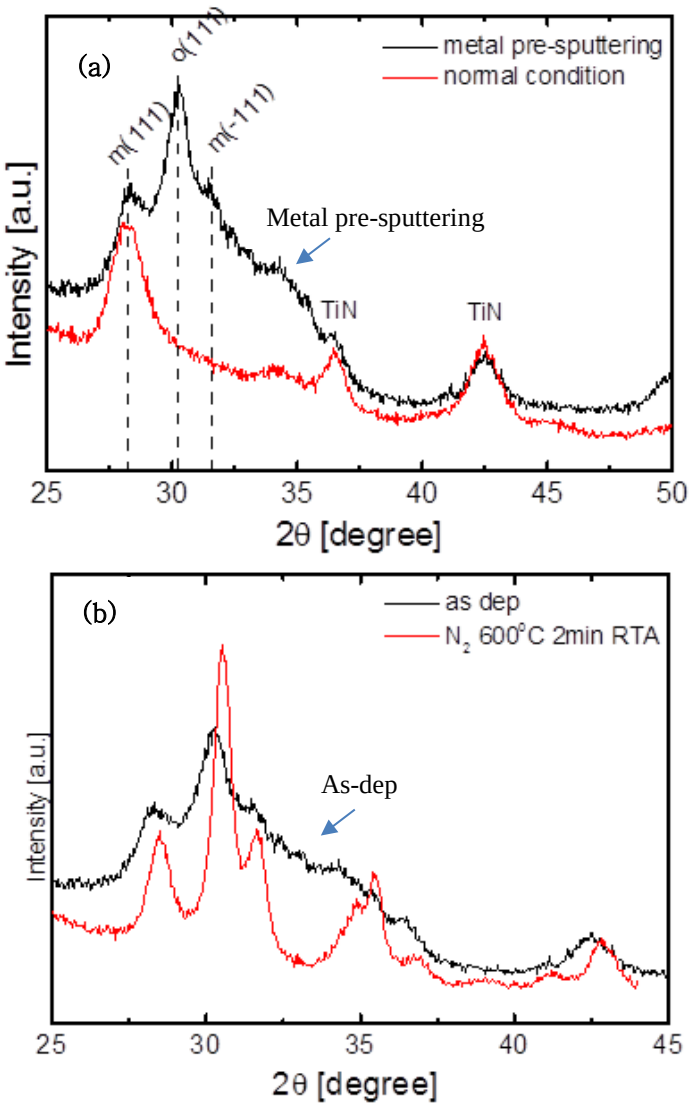

Figure 4. 4 XRD graph of $Hf_{0.5}Zr_{0.5}O_2$ thin film (a) comparing with/without presputtering of metal target before annealing and (b) before/after annealing process of presputtered $Hf_{0.5}Zr_{0.5}O_2$ thin film

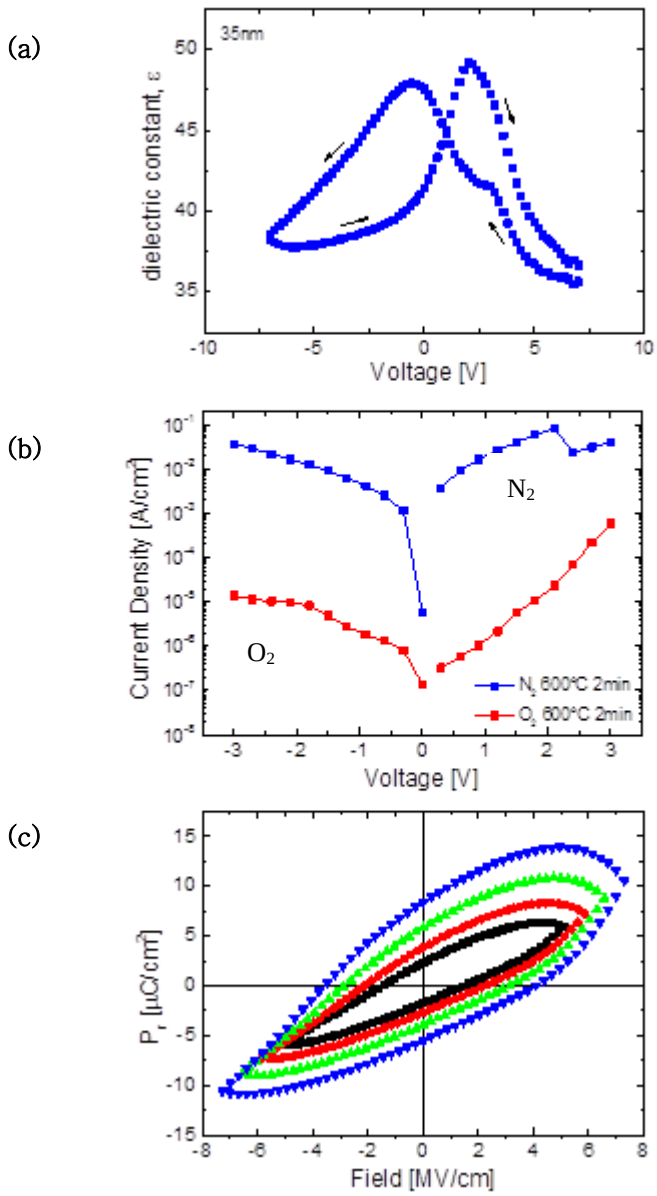

Figure 4. 5 (a) dielectric constant-voltage graph of HZO film at 35nm after annealing (b) comparison of current-voltage graph of HZO annealed at different ambience and (c) polarization-field sweeped with different voltage.

4.2. Structural Analysis

It is important that HfO_2 obtains the non-centrosymmetric lattice structure to show polarization switching residing in the fact that the ferroelectricity from the non-perovskite structure can only be realized from the non-centrosymmetric o-phase. . Therefore, confirming the formation of the o-phase is indispensable. It has been reported that HZO easily forms the o-phase on a TiN BE.[25] TiN possesses a rock salt lattice structure whereas HZO possesses a fluorite based structure. Although the reason behind why HZO shows the best ferroelectricity on TiN BE has not been fully established yet, it is within the best interest to use TiN as the TE and BE.

Fig. 4.6 (a) shows XRD data for HZO thin film deposited at high oxygen partial pressure at ~33% with m-phase under any power. It is an expected result considering the discussion in section 4.1. Hence, it can be concluded that oxygen deficient atmosphere during film deposition is favorable over oxygen rich atmosphere. Also, Fig. 4.6 (b) shows that under different power condition at 1mtorr, low power and mid-power showed some formation of the m-phase, possibly due to the slow growth rate leading to larger grain size, indicating that it is not the most favorable condition to show the best ferroelectric behavior. Therefore, high oxygen partial pressure and low, mid-power condition at low oxygen partial pressure have been ruled out for consideration.

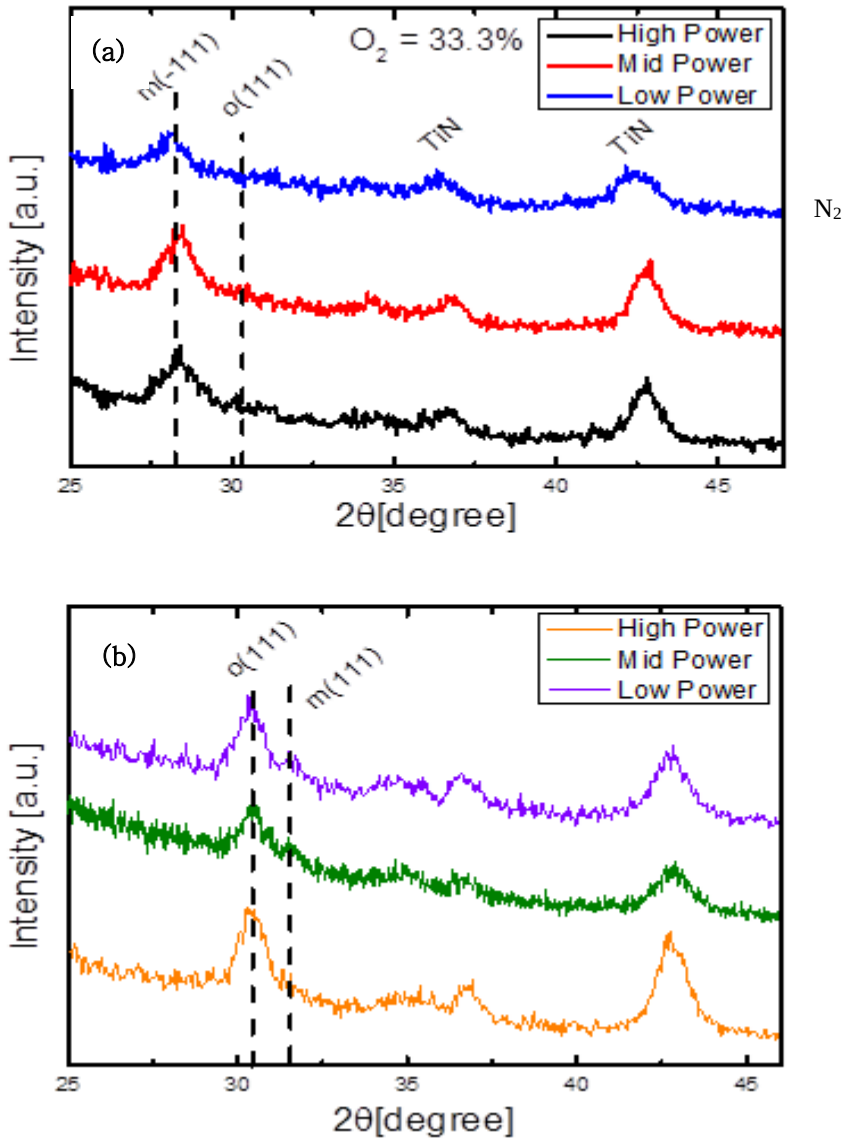

Figure 4. 6 GIXRD for HZO thin film (a) for different power under 33% oxygen partial pressure and (b) for different power at 1mtorr. (High/mid/low power starting from the top)

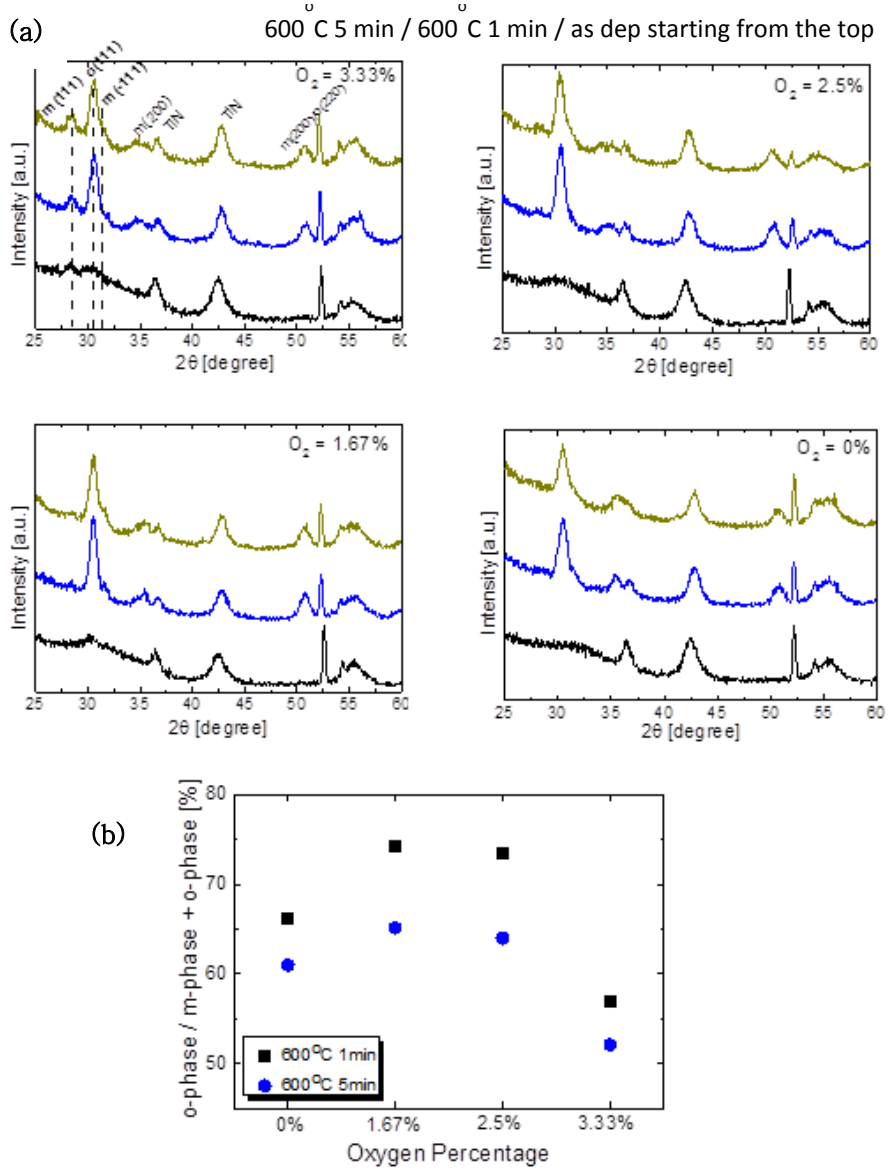

Figure 4. 7 (a) GIXRD for $Hf_{0.5}Zr_{0.5}O_2$ thin film deposited under different oxygen partial pressure and annealed for different time. (b) Comparison of o-phase percentage obtained from XRD peak intensity. As oxygen partial pressure decreases amount of o-phase increases. Annealing for 1 minute under O_2 ambience at 600°C created higher o-phase than long annealing time.

Fig. 4.7 (a) shows GIXRD data for each oxygen partial pressure condition under different annealing time. Annealing was conducted at 600^{o}C for 1 minute for all cases. It can be seen that combination of the o-phase and m-phase together with t-phase have been developed. The peak intensity varies for different oxygen partial pressure. Also, different peak formation occurs between different annealing conditions. Under certain conditions, m-phase peaks can be observed, which is expected to degrade the ferroelectricity.

The amount of the o-phase created can be conjectured by the o-phase to m-phase ratio. For comparison, peak around 30.5^{o} has been used to deduce the intensity of the t-phase and the o-phase. The reason why such 2θ position is chosen should be mentioned. Although the o-phase and t-phase possess different orientation of the plane, peaks around 30.5^{o} show peak that is large enough to distinguish from other peak and no peak overlapping occurs, which makes the comparison easy.[7] However, it is important to note that peaks for the o-phase at (111) direction and the t-phase at (011) direction almost overlap with each other, which requires separation. It has been reported that (111) o-phase has slightly lower 2θ than that of the t-phase which is also applied in this work. The characteristic peaks for m-phase were ~28.5^{o} and ~31.4^{o} for (111) and (-111) m-phase, respectively.[7]

Peaks at ~36.5^{o} and 42.5^{o} corresponds to the TiN BE and there has been a

small shift for TiN to higher 2θ position after annealing. Peak shifting towards the higher angle indicates that the d-spacing has decreased. This is an indication that TiN TE and BE have been oxidized, since N with larger atomic radius has been replaced by O with smaller radius, resulting in the volume shrinkage and smaller d-spacing. When d-spacing was calculated using (111) TiN peak, the lattice parameter of TiN before annealing was about 4.26A and 4.24A after annealing, which gives 2A d-spacing difference.

To quantitatively compare the amount of the o-phase, peak splitting was conducted using 30.4^{o} and 30.8^{o} peak for o- and t-phase, respectively. After peak splitting, the peak area of the m-phase and the o-phase are combined to get the approximate percentage of the o-phase, which could work as a parameter to explain the electrical result based on structural point of view. Fig. 4.7(b) shows that as oxygen partial pressure decreases, the intensity of the o-phase peak increases, which well coincides with electrical results shown in Section 4.3. Also, under the same oxygen partial pressure condition, annealing for 1 minute over 5 minute was more favorable to create ferroelectricity.

The o-phase percentage at 1.67% of oxygen partial pressure is the highest implying that less amount of reactive oxygen gas is more favorable for the o-phase formation. One possible explanation could be amount of resputtering. During sputtering deposition under reactive oxygen flow, oxygen ion in the

state of plasma could bombard into the film, taking away oxygen atoms that are already deposited in the film, which is called resputtering. This phenomenon could degrade the film quality, which could affect the formation of the o-phase. Another explanation would be the grain size. With more reactive gas atoms in the chamber, the deposition rate decreased. Slower deposition rate gives more time for the grain to nucleate and grow, resulting in larger grain size. Since larger grain size favors m-phase more, such result could be seen. Interestingly, when no reactive oxygen gas was used during deposition, the o-phase percentage decreased. When the GIXRD peak width at 30.5^{o} was compared (which is not shown) the peak width was thicker under 0% oxygen partial pressure, indicating that more t-phase has been formed compared to other condition. With considerably large electric field, t-phase could transform into o-phase, but since the film deposited under 0% oxygen partial pressure showed high leakage current, such large electric field condition could not be applied.

When the annealing time was elongated, it can be easily noticed that the peak intensity around 30.5^{o} decreases combined with the m-phase peak formation around 31.4^{o}. As annealing time prolonged, the nucleation process would continue which would lead to grain size growth. The grain size is closely related to the phase formation, where the larger grain size leads to the m-phase formation and this was confirmed with GIXRD data.

The in-plain strain has been calculated to verify any difference in amount of strain to induce the o-phase formation. It has been reported that more than ~1.5% in-plain strain is necessary for the phase transformation from t- to o-phase.[8] Figure 4.8 shows the in-plain strain % value for different oxygen partial pressure. The method to obtain such results is covered in depth by Park et al.[8] The change in strain % with respect to the oxygen partial pressure is relatively small and all the in-plain strain goes over 1.5% which indicates that large enough strain has been formed. In-plane strain slightly increases with decreasing oxygen partial pressure. According to W. D. Nix et al., the strain is induced in Volmer-Weber type growth and its stress is inverse of the size of the island radius.[28] Therefore, since the nuclei size under low oxygen partial pressure would be small due to fast deposition rate, the results are reasonable.

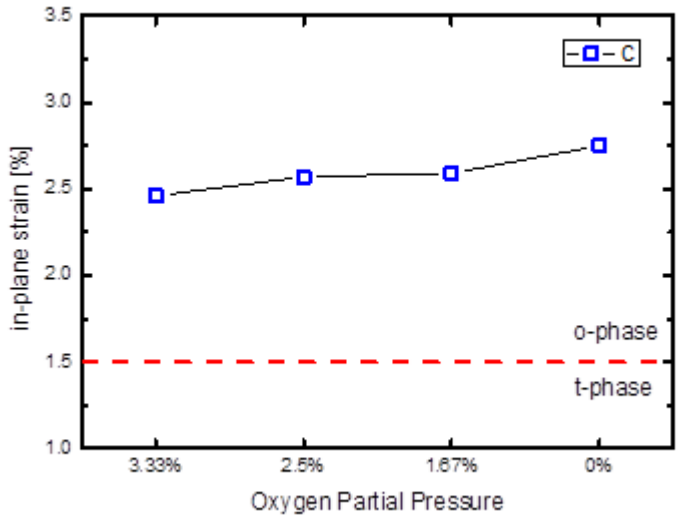

Figure 4. 8 In-plane strain calculation of HZO thin film. About 1.5% strain is the boundary for phase transformation from t-phase to o-phase.

4.3. Electrical Property

It is necessary to confirm that amount of the o-phase formation is coherent with high polarization result. Fig. 4.9 shows the obtained hysteresis curve under for different oxygen partial pressure. The wake-up was conducted to obtain saturated hysteresis curve with higher P_r value. Wake-up is the phenomenon in which the increase in P_r is observed when field cycling is conducted to the ferroelectric film. Considering that PZT showed fatigue behavior when field was cycled over 10^6, it is an interesting and unique merit of HZO to show such behavior. Many results have been reported regarding wake-up effect[29] and hence, further explanation is omitted.

Fig 4.9 (d) shows a clear antiferroelectric-like behavior at the pristine state, which was not observed when the film stoichiometry was 1:1, prepared by ALD method. According to M. Pesic et al., oxygen vacancy concentration stabilizes the t-phase.[30] Under high electric field, t-phase transforms to o-phase which then changes to t-phase again at low electric field, resulting in antiferroelectric behavior. Therefore, antiferroelectric behavior under 0% oxygen partial pressure at the pristine state could be the indication of large oxygen vacancy concentration. As the wake-up occurs after 10^6 field cycling, the full hysteresis is formed with higher P_r and E_c, which is a typical wake-up behavior. After the wake-up, the hysteresis curve shows different slope and shape for each oxygen partial pressure condition. For HZO deposited under 0% oxygen partial

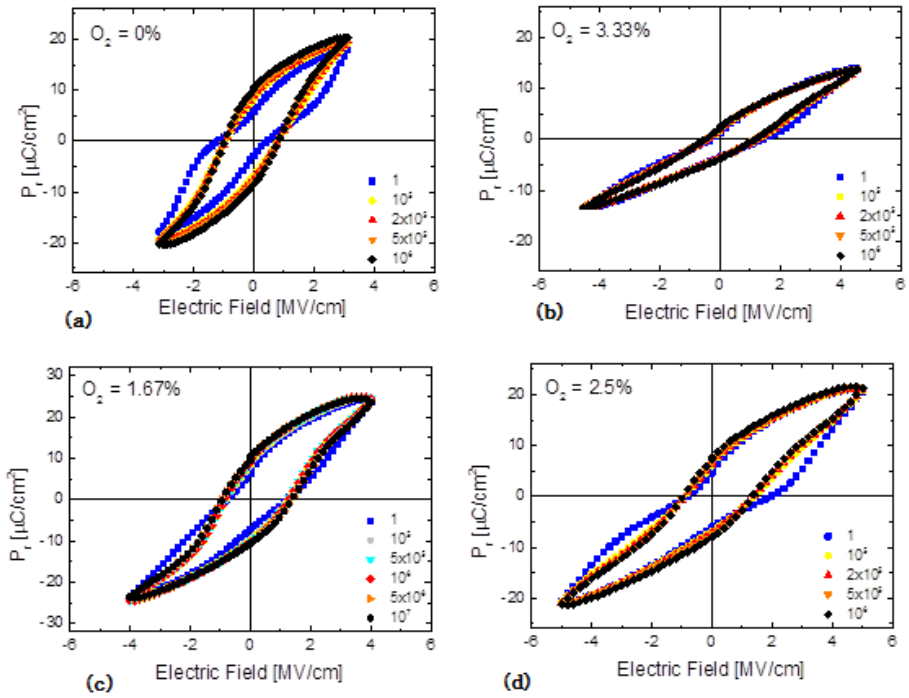

Figure 4. 9 Hystersis loop for HZO thin film under different oxygen partial pressure at the pristine state. The field cycling was conducted for ~10^6 and the wake-up effect was observed.

pressure, large electric field could not be applied due to the poor leakage current behavior.

Fig. 4. 10 shows P-E data under different annealing time. As the amount of oxygen partial pressure decreases, it can be easily seen that the slope of the hysteresis curve gets steeper with increasing remnant polarization value. Higher slope value indicates the more uniform coercive field distribution to switch the polarization easily under the same voltage and is beneficial for ferroelectric applications.

To facilitate the process of comparing the $2P_r$ value for each oxygen partial pressure, separate data have been plotted in Fig. 4.11. The sample that was deposited under 0% O_2 partial pressure with 600^oC thermal annealing for 5 minutes was not included in the data since it had high leakage to acquire the hysteresis curve. From the given data, it is clear that $2P_r$ value increases with decreasing oxygen partial pressure, which is in accordance with GIXRD data discussed in Section 4.2 and also shown again in Fig. 4.11 for comparison.

Few possible explanations could substantiate the obtained results. One of the possible explanations could be the involvement of oxygen anion re-sputtering. As the oxygen partial pressure increases, the amount of oxygen anion would increase, bombard more frequently towards the substrate and take out the

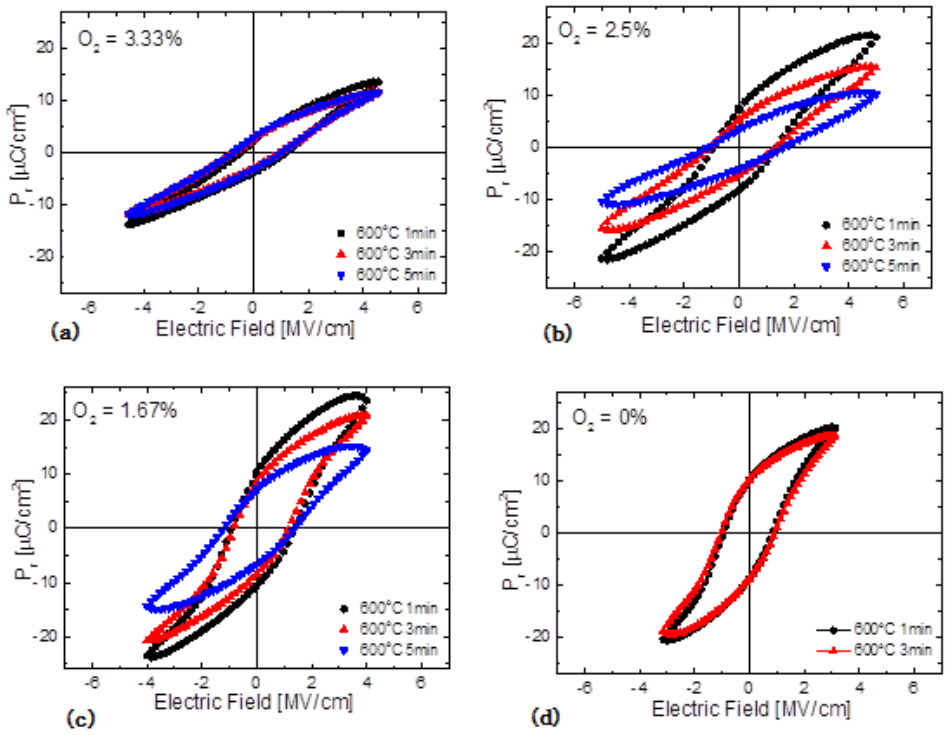

Figure 4. 10 Hystersis loop for HZO thin film deposited at different oxygen partial pressure and annealed for various time.

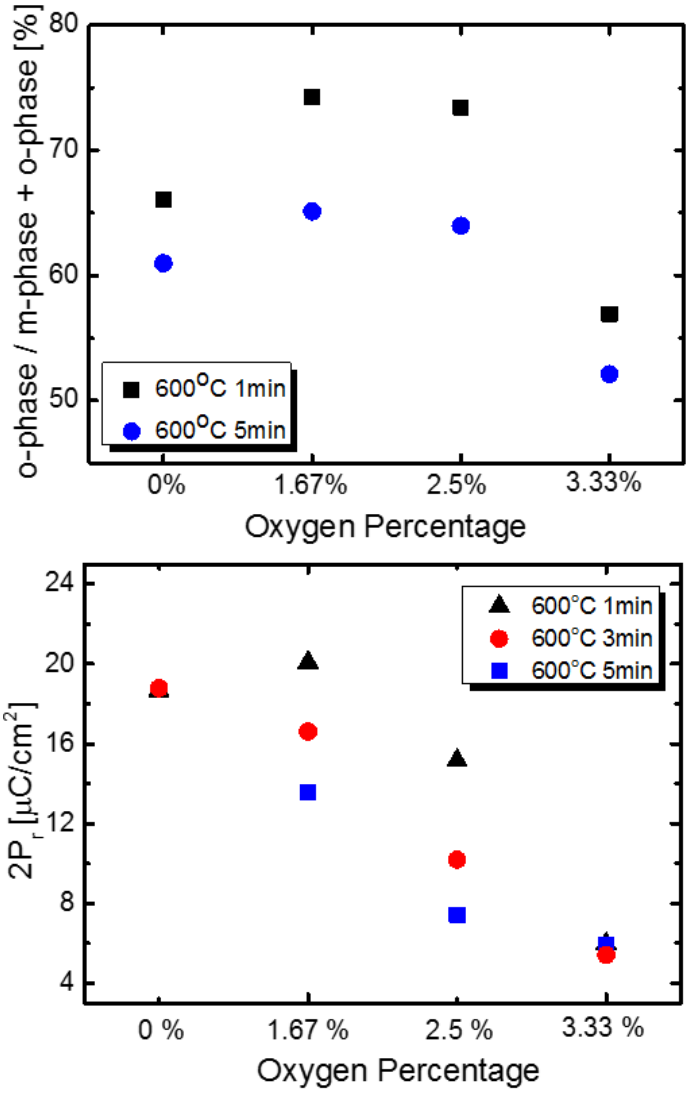

Figure 4. 11 Remanent polarization values have been plotted for different annealing time at different oxygen percentage. O-phase % graph, which was already shown in Fig. 4.7, has been inserted for comparison

that is already deposited on the film. This would create the oxygen vacancy and change the stoichiometry of the film, which could again affect the phase or electrical current behavior. Hence, it is reasonable that less oxygen partial pressure is more favorable to produce enhanced quality thin film, which again leads to superior ferroelectric property.

It is interesting to note that under the same temperature value, less annealing time leads to higher $2P_r$ value for all oxygen partial pressure cases. As the annealing time increases, the nucleation proceeds further which would result in larger grains. Surface energy effect could explain the obtained results that higher grain size would result in the formation of the m-phase. The formation of the o-phase is limited to certain high-pressure (or anisotropic-strain), and the metastable t-phase ($P4_2/nmc$) can be stable over the m-phase ($P2_1/c$).[7] Surface energy of the t-phase is lower than that of the m-phase, which would make the t-phase more stable when the film is thin with smaller grain size than thicker films with larger grain size.

Another explanation would be TiN electrode oxidation. When the annealing temperature was too high (not shown in the data) or when the annealing time was too long, TiN TE and BE, which is vulnerable to oxidation, would oxidize too much that oxide film thickness would be too thick. This addition of oxide layer would decrease the field applied to ferroelectric layer, which would then

decrease the polarization value. Such results can be seen in Fig. 4.12, where comparison of the P-V data for different annealing temperature is shown. Low annealing temperature (500^{o}C) might have resulted in not enough crystallization leading to less nucleation and growth behavior.

Fig. 4.13 (a) shows dielectric constant-voltage graph for different oxygen partial pressure. Two peaks can be seen to indicate that polarization switching is occurring. It can be seen that dielectric constant under low oxygen partial pressure case is much higher than that of high oxygen partial pressure case. Considering that the dielectric constant is ~20 and ~35 for m-phase and t-phase, respectively, it can be deduced that high oxygen partial pressure condition induces higher m-phase formation which lies along the structural and XRD analysis. On the other hand, it can be said that oxygen deficient condition induces more of t- or o-phase formation that leads to higher dielectric constant. The dielectric constant value is extracted from capacitance-voltage graph at the highest voltage where the full switching occurred to avoid any confusion with background dielectric constant, switching, or defect movements. The dielectric constant is not different by much when compared with HZO deposited at 0% and 1.67% oxygen partial pressure. Fig. 4.13 (b) shows the combination of both dielectric constant and P_r value with respect to different oxygen partial pressure. As oxygen partial pressure increases, the dielectric constant decreases, indicating the formation of the m-phase, which can also be represented as

decrease in $2P_r$ value.

After power, oxygen partial pressure, and annealing temperature were optimized to produce the best characteristics, it was necessary to optimize the annealing time. Fig. 4.14 shows the current-voltage curve depending on the annealing time variance under O_2 ambience. When the film underwent thermal annealing process under N_2 ambience, which is usually the case for HZO thin film deposited by ALD, the leakage problem could not be solved. Hence, all the thermal annealing process was conducted under O_2 ambience to rectify the leakage problem. It can be seen from the figure that too short of annealing time does not solve the leakage problem and too long of annealing time only leads to limited current-voltage behavior. Considering the previous discussions regarding TiN electrode oxidation, annealing for long time is not favorable for optimization of the film deposition. From the graph, it can be deduced that annealing time of about 1 minute to 3 minutes showed the best result, and considering the fact that 3 minutes showed less $2P_r$ than that with 1 minute annealing time, it can be concluded that 1 minute rapid thermal annealing under O_2 ambient is the most optimized annealing condition.

It can be also seen that higher current values are formed when the film is biased by the same positive voltage as that of the negative voltage, which implies that the BE-ferroelectric film interface quality is worse than the interface with the TE. This can be also confirmed from the P-V data that the

graph is a bit positively shifted to positive side, which implies that there are defect charges near the BE that hinders the injection of electron from the bottom side of the film which deters the polarization switching. The quality of the bottom interface between the oxide film and the BE could be affected during the sputtering of oxide film due to its intrinsic mechanical bombardment effect which could degrade the interface quality upon deposition. However, the same effect could arise during the TE, and therefore, the way to avoid interface traps or other defects near interface during sputtering needs to be considered.

Table 4.1 summarizes the optimized power, oxygen partial pressure, working pressure, and annealing condition to deposit ~11nm thickness of HZO thin film using RF magnetron sputtering.

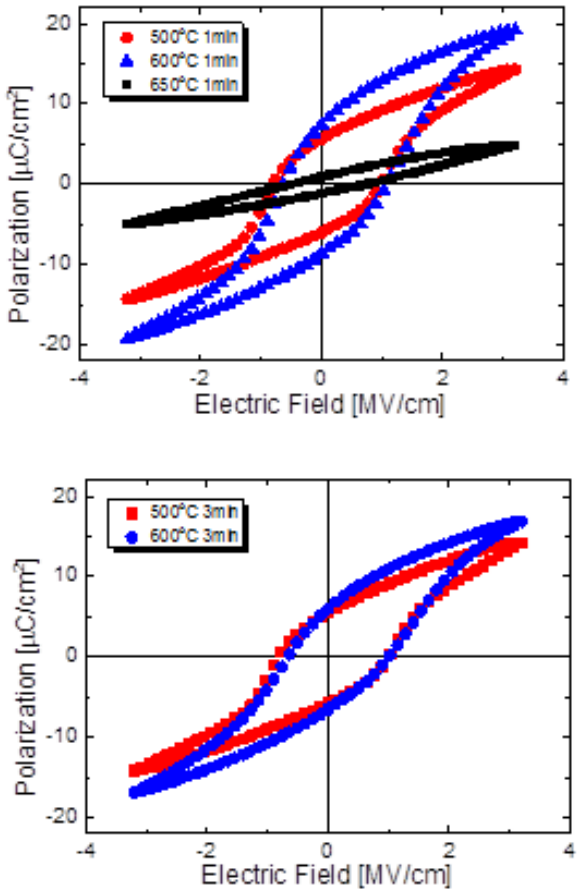

Figure 4. 12　Hysteresis loop for HZO thin film with different annealing temperature and time

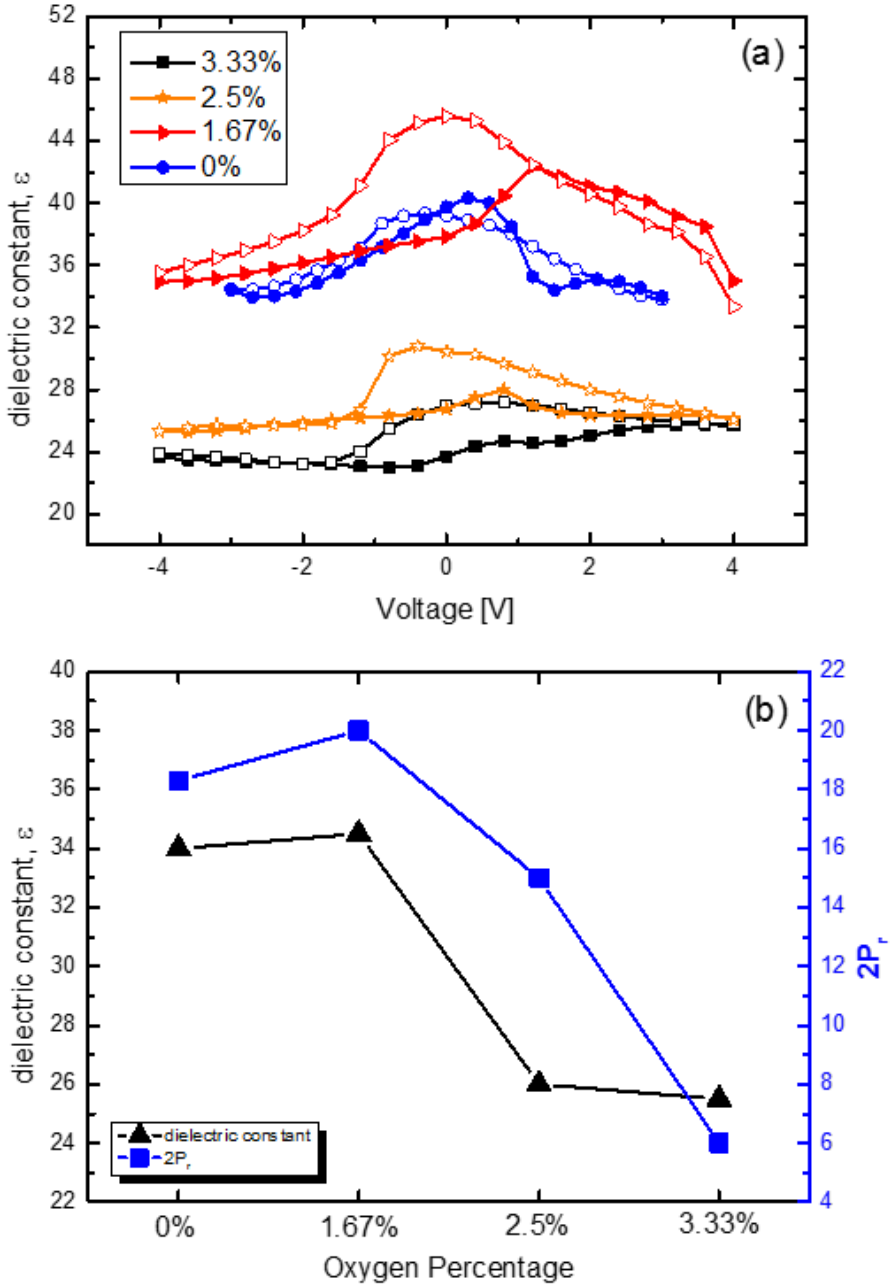

Figure 4. 13 (a) Dielectric-voltage graph for different oxygen partial pressure and (b) comparison bewteen dielectric constant and $2P_r$

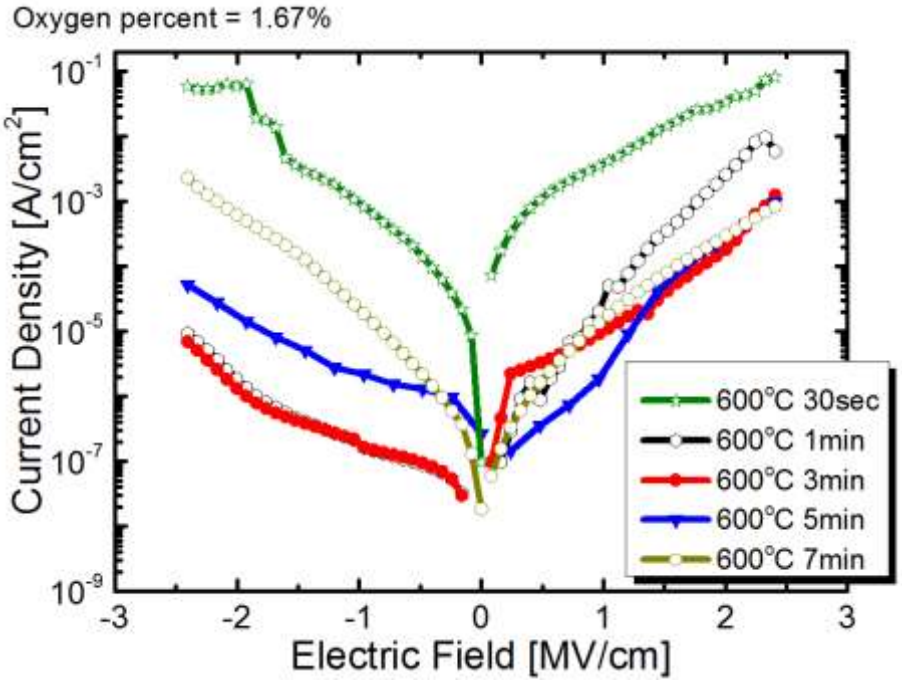

Figure 4. 14　Current density-electric field of HZO thin film annealed for different duration of time.

Factors	Result
Power (HfO_2/ZrO_2)	135/190W
Ar:O_2	0%
Annealing condition	O_2
	600ºC
	1min
Working pressure	1mtorr

Table 4. 1 Summarized optimized condition when depositing ~10nm HZO thin film using RF sputtering at room temperature.

4.4. Morphology

Sputtering is a physical vapor deposition method where the particles from the target physically bombard the substrate as they are deposited. As a result, compared to chemical vapor deposition, where the source in gas phase is chemically bonded to the substrate and get deposited, sputtering can damage the film quality. At more or less 10nm thickness, the film quality can be degraded due to the harsh bombardment condition, which can affect the electrical property.

Fig 4.15 and Fig 4.16 shows the SEM top-view image and the atomic force microscopy (AFM) image of the 11nm HZO thin film before thermal annealing. From the SEM image of the top-view of the film, the grain size can be deduced. Fig 4.17 shows the comparison of the grain size with respect to the oxygen partial pressure before and after the annealing process. As oxygen partial pressure decreases, the average grain size also decreases. The average grain size is 13.8nm, 13.4nm, 12.6nm, and 11.2nm for 3.33%, 2.5%, 1.67% and 0%, respectively, and increase by a little after annealing, but not over the critical grain size for phase transition. This phenomenon can be well understood from the deposition rate perspective. As the amount of reactive gas decreases, there are less amount of gas particles in the medium between the target and the substrate. As result, the mean free path of the target particle increases and the

deposition rate increases more quickly. When the deposition rate is high, there is not enough time for nucleation to happen before another particle gets deposited. Therefore, smaller grains are formed, which coincides with the experimental results.

This again aids in understanding the reason of higher polarization value under lower oxygen partial pressure. As smaller grain size is formed, t- phase is much more easily formed compared to the m-phase due to the surface energy consideration.[19] Also, there has been a report about the relationship between the thickness of the film and the polarization value.[7] As film thickness gets thicker, the polarization value decreases. As the film thickness increases, the grain size will evolve to a greater size of the grain which facilitates the formation of the m-phase. Therefore, it can be understood from the data that the faster the deposition rate, the smaller the grain size, which helps to produce more o-phase leading to higher polarization value.

AFM images of the HZO thin film were obtained using the non-tapping mode. The grain size can be hardly measured from the image because the tapping mode does not directly contact the surface and therefore creates the bigger grain image than the size of the real grain. The roughness R_q value was calculated to be 0.62nm, 0.58nm, 0.5nm, 0.48nm for oxygen partial pressure of 0%, 1.333%, 2.5%, 3.33%, respectively, indicating that the film has been deposited uniformly.

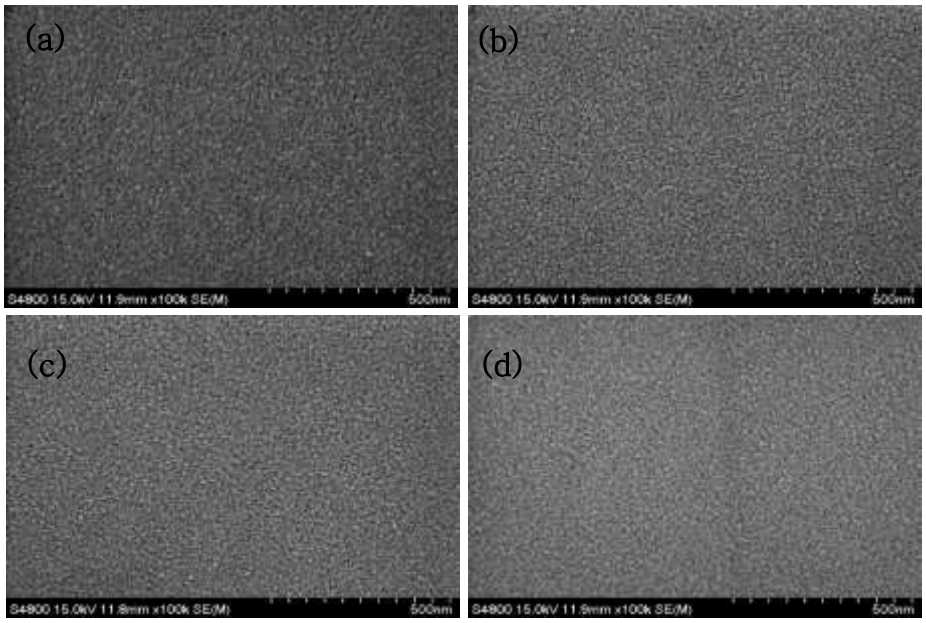

Figure 4. 15 SEM image of HZO thin film before annealing deposited under (a) 3.33% (b) 2.5% (c) 1.67% and (d) 0%

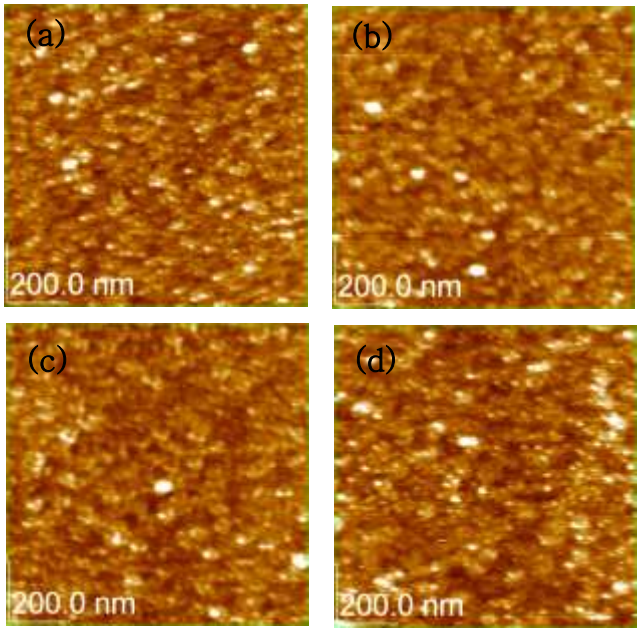

Figure 4. 16　AFM image of HZO thin film before annealing deposited under (a) 3.33% (b) 2.5% (c) 1.67% and (d) 0%

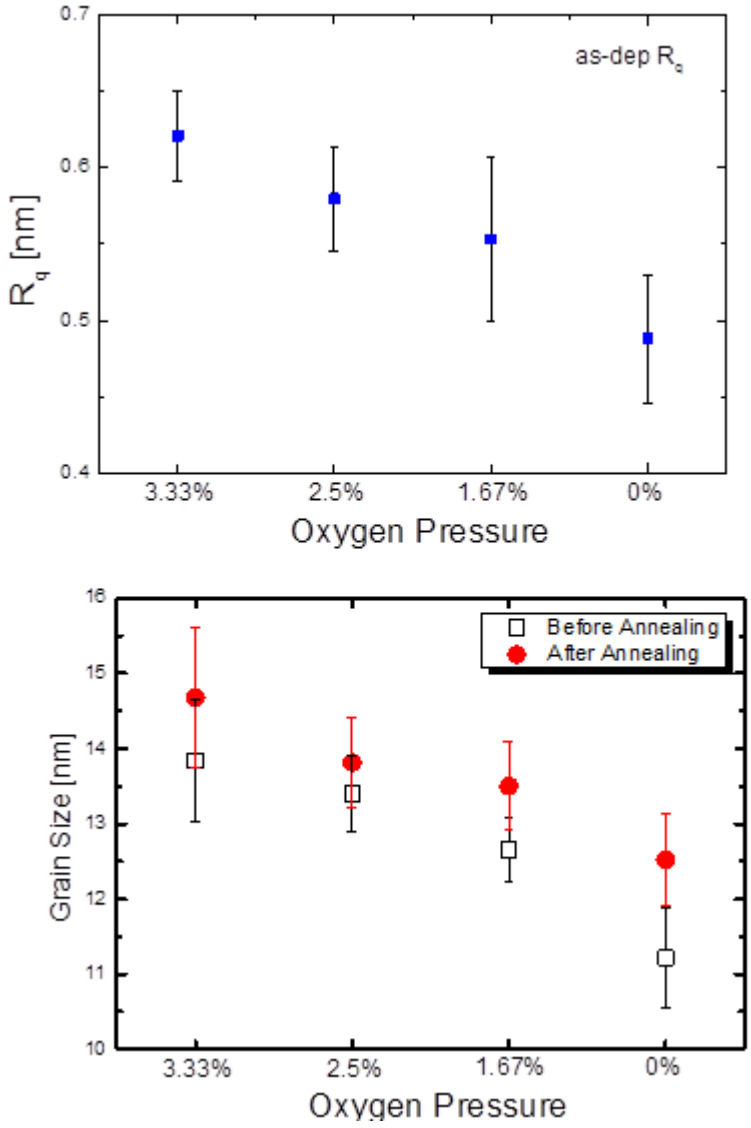

Figure 4. 17 RMS and grain size for HZO thin film before annealing.

Grain size before / after annealing is also plotted.

The figure shows that the roughness of the film decreases with decreasing oxygen partial pressure, although the difference between the values are quite small.

After thermal annealing, the roughness increased due to the abruptness of the surface (results not shown). This abruptness with a spherical shape on the surface of the film seems to be the hillock formation. The formation of the hillock was present with or without the TE (results not shown as AFM images) and was confirmed from the top view of the SEM image in Fig. 4.18 and the cross-sectional image before and after annealing in Fig. 4.19 (a) and (b), respectively. Before annealing, the film surface was smooth although the HZO film layer can hardly be distinguished due to the low magnification compared to transmission electron microscopy (TEM). After thermal annealing under oxygen atmosphere, however, small voids between the TiN BE and SiO_2 substrate were sporadically formed and this affected the whole morphology of the film. Again, since the thickness of the HZO film is thin, it is difficult to observe the contact layer between the oxide film and the electrode.

It is expected that these voids originated from nitrogen gas which evaporated from TIN BE during O_2 annealing due to TiN BE oxidization or Ti adhesion layer oxidation, and seemed to push up the layer, causing structural deformation. The size and the density of these hillocks varied depending on the oxygen

partial pressure. As the oxygen partial pressure decreased, the size of the hillocks gets smaller with higher density. It is interesting to note that the very voids were not produced under nitrogen annealing procedure as can be seen in Fig 4.19 (c). Also, none of the voids formation were reported for HZO film deposited by ALD. Since these voids do not seem to affect the polarization switching but rather only affect the leakage current behavior, further investigation was not conducted.

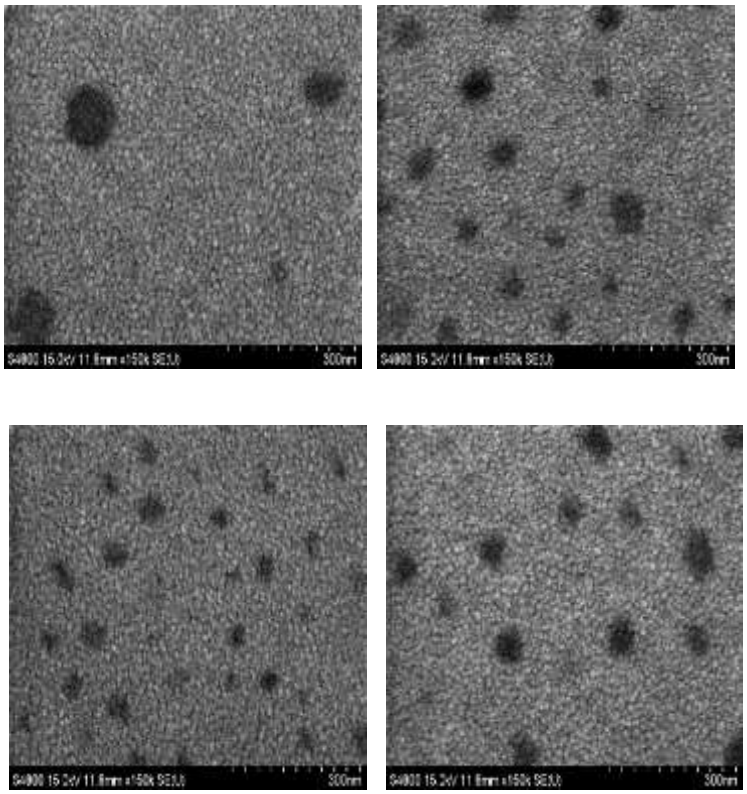

Figure 4. 18 Top view image of HZO thin film after annealing in O_2 ambience at 600°C for 1min. Oxygen partial pressure was 3.33%, 2.5%, 1.67%, and 0%, starting from the left top corner and clockwise.

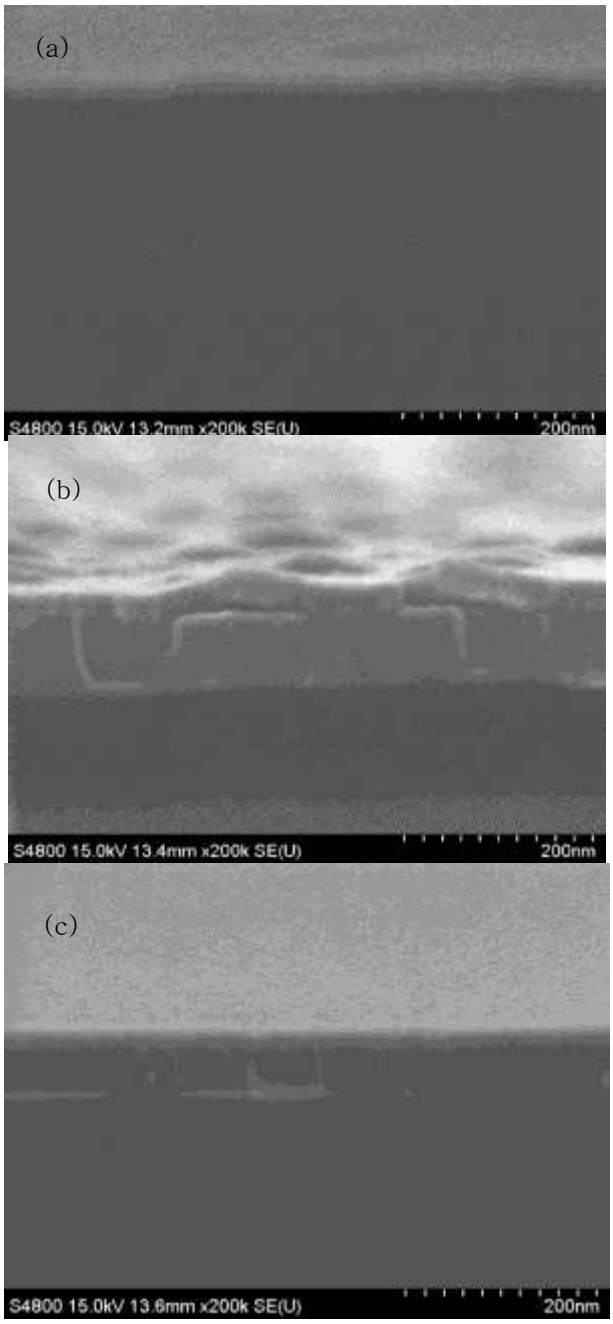

Figure 4. 19 Cross-sectional image of HZO thin film (a) before annealing and after annealing in (b) O_2 and (c) N_2 ambience.

4.5. Chemical Analysis

Fig. 4.20 shows the auger electron spectroscopy (AES) depth profiles of the 11nm HZO thin film deposited under 1.33% oxygen partial pressure before and after the thermal treatment. Before annealing there seems to be less oxygen atoms diffusion into the BE compared to the TE. It is interesting that oxygen atoms are present only at the TiN TE. Considering that TiN is a material which readily oxidizes, oxygen concentration near the TE can be well understood. Less amount of oxygen atoms could be due to the already present native oxide layer of bottom TiN electrode which prevented further oxidation of TiN itself. After thermal treatment, due to the annealing condition under oxygen ambient, the concentration of the oxygen atoms is high for both TE and BE. It is also known that TiN readily oxidizes by post-heat treatment under oxygen ambience.[21]

Fig 4.21 shows X-ray photoelectron spectroscopy (XPS) data for 11nm HZO thin film deposited under different oxygen partial pressure before and after thermal treatment. The Ar^+ etching was not conducted to prevent the difference in the amount of etching. Strong C-C bonding peak of the C 1s was set at 285eV, and other peaks are calibrated. XPS peaks for O 1s spectra can be split into C-O bonding which is at ~532eV and other oxygen peaks. Since Hf- O and Zr-O for HfO_2 and ZrO_2 overlap with each other, it was difficult to have two distinct peaks. Therefore, only relative peak positions were compared for different

Oxygen : 1.67%

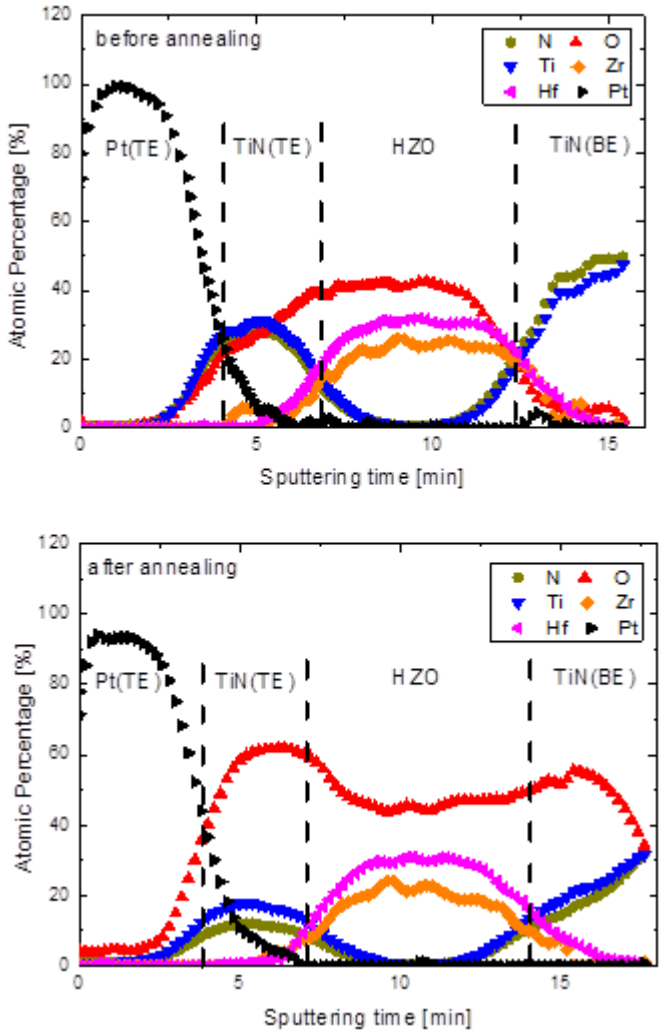

Figure 4. 20 AES data for HZO thin film before and after annealing for HZO thin film deposited under 1.67% of oxygen partial pressure

oxygen partial pressure cases.

The peak position and the intensity of the peak are nearly similar to each other, indicating that the peak shift or intensity comparison of O 1s peak is meaningful. One representative peak was given to combined HfO_2 and ZrO_2 due to difficult peak splitting, and only the binding energy shift was considered. Fully oxidized HfO_2 or ZrO_2 should have binding energy at about 530.5eV. However, the representative peak for O 1s is far from the fully oxidized position for the as-dep film, indicating that the stoichiometry for the as-dep film is not 1:2. It is necessary to acquire the film with full stoichiometry since partial oxidized state represents the formation of oxygen defect, which could result in ferroelectric behavior degradation. As the partial pressure decreases, the O 1s peak shifts toward the fully oxidized BE indicating less oxygen partial pressure is favored in terms of stoichiometry perspective.

Hf 4f peak and Zr 3d peak were also plotted. However, the peak splitting was not easy because the film possessed different Hf and Zr binding condition. It was necessary to only consider the binding energy shift was considered for both cases. As the oxygen partial pressure decreased, Hf 4f peak shifted towards the fully oxidized binding energy peak, which coincides with the oxygen peak shift result. The same trend was also observed for Zr 3d case. Fully oxidized binding energy was far from the binding energy from the as-deposited film and less

oxygen partial pressure was more favorable when preparing more oxidized film. The probability of peak shifting from sample charging can be omitted since when the width of the peak was compared, different peak width under oxygen partial pressure showed different width indicating that the bonding state is different for each condition.

Also, the local valley intensity between the satellite peaks is different for different oxygen partial pressure conditions. When the Gaussian-Lorentzian fitting was conducted, narrower peak was easily fitted with one fully oxidized HfO_2 or ZrO_2 peak. Wider peak required additional peak for the fitting indicating that wider peak possessed more different bonding states. Narrower peak was observed under no oxygen partial pressure and indicates more favorable deposition condition, which also lies with binding energy shift argument.

After annealing, HZO films deposited with oxygen reactive gas showed almost uniform peak binding energy, indicating that the oxygen atoms or other target clusters diffused to the stable position within the film. Since annealing process enhances the structural damage or other undesired bonding states, the same effects probably occurred. The film deposited under no oxygen reactive gas was not aligned since it was less oxidized compared to other samples by having smaller binding energy. Considering the smaller binding energy for

more metallized state together with the current-voltage behavior, the result seems probable.

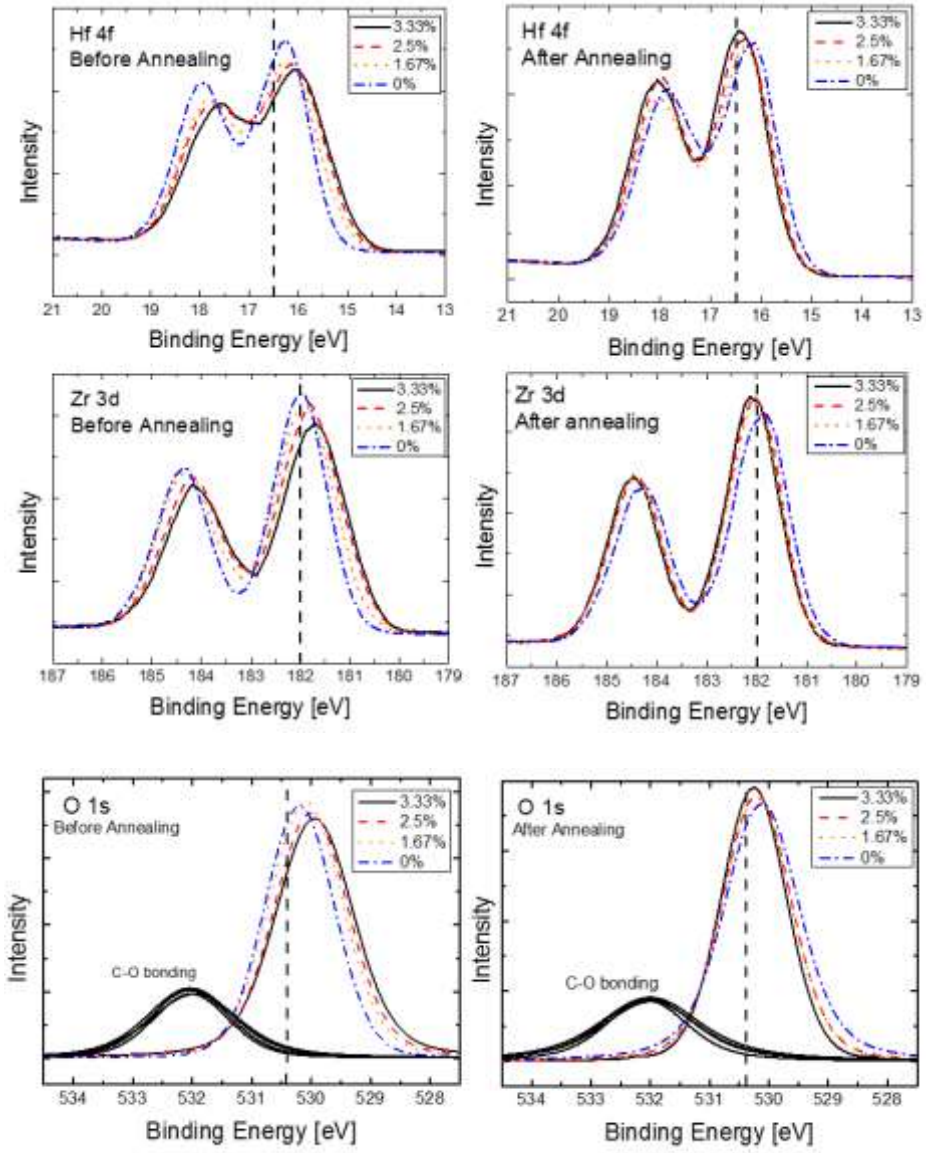

Figure 4. 21 XPS data for Hf 4f, Zr 3d, and O 1s before and after annealing deposited under different oxygen partial pressure

5. Conclusion

In conclusion, the physical and ferroelectric properties of HZO films prepared by RF sputtering method under different deposition conditions were studied systematically. HZO films can show a feasible ferroelectricity with $2P_r$ of ~20μC/cm^2 on a TiN bottom electrode at a thickness of ~11nm. Various sputtering conditions like the target power, working pressure, oxygen reactive gas partial pressure influenced the film property, and also, the annealing ambience, time, and temperature affected film quality. Film thickness and stoichiometry were other influential factors which were set as fixed values. The sputtering conditions were optimized and the most favorable ferroelectric phases are determined to arise at 135W and 190W for HfO_2 and ZrO_2 power, respectively, 1mtorr of working pressure and 0% of oxygen reactive gas partial pressure. It is then necessary to be annealed under O_2 ambience at 600^{o}C for 1 minute.

It seems that the conditions mentioned intermingled to change the grain size of the film, which determine the surface energy and the most stable phase at which the film is formed. Although there are many factors to induce the ferroelectric phase of thin film including effects from top and bottom electrodes, oxygen vacancies and in-plane strain and stress within films, it seems that grain size which is closely related to surface energy effect is the most influential

factor to determine ferroelectricity of HZO thin film prepared by RF sputtering method. These findings support the previously suggested mechanism of the evolution of the ferroelectric phase in the HZO film: the surface energy effect to induce the phase transformation from m- or t-phase to o-phase.

Reference

[1] N. Setter et al., J. Appl. Phys. 100, 51606 (2006)

[2] J. Hoffman, et al., Adv. Mater. 22, 2957 (201)

[3] H. Koike, U. S. patent no. 5600587 (1997)

[4] M. H. Park et al., App. Phys. Lett., 104, 072901 (2014)

[5] T. P. Ma et al., IEEE Electron Device Lett. 23, 386 (2002)

[6] D. S. Jeong, et al., Rep. Prog. Phys. 75, 076502

[7] M. H. Park et al., App. Phys. Lett., 102, 242905 (2013)

[8] M. H. Park et al., App. Phys. Lett., 104, 072901 (2014)

[9] T. S. Boske et al., App. Phys. Lett., 99, 102903 (2011)

[10] S. Muller et al., Adv. Funct. Mater., 22, 2412 (2012)

[11] J. Muller et al., Nano Lett., 12, 4318 (2012)

[12] J. Muller et al., ECS J. Solid State Sci. Technol. 1, N123 (2012)

[13] C. K. Lee et al., Phys. Rev., B78, 012102 (2008)

[14] D. K. Maurya et al., coatings, 4 (4), (2014) 756-771

[15] Prof. Kim Hyung Joon's lecture note

[16] J. Perez de la Cruz et al., J. Appl. Phys., 108, 114106 (2010)

[17] J. E. Lowther et al., Phys. Rev. B, 60, 14485 (1999)

[18] E. H. Kisi et al., J. Am. Ceram. Soc., 81, 741 (1998)

[19] M. Shandalov et al., J. Appl. Phys., 106, 084322 (2009).

[20] M. Hoffmann et al., J. Appl. Phys., 118, 072006 (2015)

[21] T. Shimizu et al., Appl. Phys. Lett. 106, 112904 (2015)

[22] T. Shimizu et al., Jpn. J. Appl. Phys., 53, 09PA04 (2014)

[23] M. H. Park et al., Phys. Status Solidi RRL 8, No. 6, 532-535 (2014)

[24] M. H. Park et al., App. Phys. Lett., 102, 112914 (2013)

[25] M. H. Park et al., App. Phys. Lett., 105, 072902 (2014)

[26] Schroeder, ISAF, 2015, Singapore

[27] S. K. Kim et al., Electrochem. Solid State Lett. 11, G9 (2008)

[28] W. D. Nix et al., J. Mater. Res. 14, 3467 (1999).

[29] H. J. Kim et al., Nanoscale, 8, 1383-1389 (2016)

[30] Pešić, M. et al., "Physical Mechanisms behind the Field-Cycling Behavior of HfO2-Based Ferroelectric Capacitors. Adv. Funct. Mater. 2016

List of publications

1. Refereed Journal Articles (SCI)

1.1 Domestic

1.2. International

1. Han Joon Kim, Min Hyuk Park, Yu Jin Kim, **Young Hwan Lee,** Woojin Jeon, Taehong Gwon, Taehwan Moon, Keum Do Kim, and Cheol Seong Hwang, "Grain size engineering for ferroelectric $Hf_{0.5}Zr_{0.5}O_2$ films by an insertion of Al_2O_3 interlayer", Applied Physics Letters, 19, 105, 192903 (2014)
2. Min Hyuk Park, **Young Hwan Lee**, Han Joon Kim, Yu Jin Kim, Taehwan Moon, Keum Do Kim, Johannes Müller, Alfred Kersch, Uwe Schroeder, Thomas Mikolajick and Cheol Seong Hwang, "Ferroelectricity and Antiferroelectricity of Doped Thin HfO_2-Based Films", Advanced Materials, 11, 27, 1811-1831 (2015)
3. Min Hyuk Park, Han Joon Kim, Yu Jin Kim, Taehwan Moon, Keum Do Kim, **Young Hwan Lee**, Seung Dam Hyun and Cheol Seong Hwang, "Study on the internal field and conduction mechanism of atomic layer deposited ferroelectric $Hf_{0.5}Zr_{0.5}O_2$ thin films", Journal of Materials and Chemistry C, 3, 6291-6300 (2015)

4. Min Hyuk Park, Han Joon Kim, Yu Jin Kim, **Young Hwan Lee**, Taehwan Moon, Keum Do Kim, Seung Dam Hyun and Cheol Seong Hwang, "Study on the size effect in $Hf_{0.5}Zr_{0.5}O_2$ films thinner than 8 nm before and after wake-up field cycling", Applied Physics Letters, 19, 107, 192907 (2015)
5. Yu Jin Kim, Min Hyuk Park, Woojin Jeon, Han Joon Kim, Taehwan Moon, **Young Hwan Lee,** Keum Do Kim, Seung Dam Hyun, and Cheol Seong Hwang, "Interfacial charge-induced polarization switching in Al_2O_3/Pb(Zr,Ti)O_3 bi-layer", Journal of Applied Physics, 22, 118, 224105 (2015)

Abstract (in Korean)

HfO_2 물질의 강유전성을 이용한 다양한 device application 들이 있다. 긴 역사를 갖는 FeRAM 을 서두로 transistor에서 활용되는 FeFET 이나 capacitance boost 를 야기하는 Negative Capacitance Effect, 또는 터널링을 이용한 Ferrolectric Tunnel Junction 등이 있다. HfO_2 물질에서 강유전성을 나타내는 요인으로 비대칭적인 orthorhombic phase ($Pca2_1$) 형성을 이유로 들 수 있다. 일반적으로 상유전체 상인 monoclinic, tetragonal, cubic phase 와는 달리 이런 orthorhombic phase 가 형성되기 위해서는 특정 조건이 갖추어져야 하는데 외부적인 요인, 즉 quenching 으로 인한 stress나 doping 이 가해질 때 tetragonal phase 에서 orthorhombic phase 로 상전이를 일으킬 수 있다.

박막에서 orthorhombic phase를 좀 더 안정화 시키는 요인으로는 여러 가지가 있는데 grain size 로 인한 surface energy effect, oxygen vacancy contribution, 그리고 물리적인 stress 등을 중요 변수로 생각하였고 RF sputtering 공법을 이용하여 이런 변수들을 조절 할 수 있을 때 가장 이상적인 HfO_2 박막을 만들 수 있을 것이다. 많은 dopant를 이용해 만든 박막에 대한 문헌들이 많이 있었지만 조성 범위가 넓은 Zr을 dopant로 사용하였고 박막 두께가 ~10nm 일 때 가장 좋은 특성을 보여준 문헌 연구를 토대로 실험하였다.

RF sputter 사용 시 많은 공정 변수들이 있는데 크게 박막 증착 시 공정 변수와 열처리 시 공정 변수를 나누었다. 또한 각각의 변수를 크게 세 범위로 나눠 가장 좋은 증착 조건을 형성 하였다. 135W/190W = HfO_2/ZrO_2 의 높은 파워를 사용하여 공정 압력은 가장 낮은 1mtorr로 고정 시키고 산소 분압을 3.3%, 2.5%, 1.67%, 그리고 0%로 나누어 실험을 진행하였고 deposition rate 가 판이하게 달라서 grain size 에 영향을 주었다. 결과적으로 grain size 가 작을 때 surface energy effect 효과에 의해서 monoclinic phase 가 불안정하게 형성되고 이것이 Zr 이 도핑된 HfO_2 박막의 강유전성 구현에 영향을 주었다. 또한 in-plane strain 을 계산한 결과 orthorhombic phase 형성에 영향을 미치지 않을 정도로 큰 strain 이 걸리는 것을 확인 하였고 산소 열처리 전 후 XPS 결과를 확인 해 본 결과 열처리 후 박막의 oxygen vacancy 양이 미미하게 있을지는 모르나 그 차이는 크지 않은 것으로 판단 하였다. 따라서 grain size로 인한 surface energy effect 및 stress가 가장 큰 영향을 준 변수로 생각이 되고 누설전류 특성을 고려 하였을 때 HfO_2/ZrO_2 파워 135/190W, 산소분압 1.67%, 공정압력 1mtorr, 그리고 산소 열처리를 600ºC에서 1분동안 하였을 때 ~20 μ c/cm^2 에 가까운 $2P_r$ 값을 확보 하였다.

주요어: HfO_2, ZrO_2, RF sputtering, 강유전체, oxygen vacancy, 산소 분압, 전극 산화, surface energy effect, grain size

학번: 2014-22540

이 영 환